

POLITECNICO DI TORINO

MASTER THESIS

DOUBLE DEGREE UNIVERSITY PARIS-DIDEROT - POLITECNICO DI TORINO

Microrheology of Actin Networks

Author:

Mathieu LE
VERGE-SERANDOUR

Supervisor:

Dr. Herve TURLIER



Contents

1	Introduction	2
2	Single filament study	6
2.1	Equilibrium properties	6
2.1.1	Discrete chain model	6
2.1.2	Partition function	7
2.1.3	Langevin equation	7
2.2	Definitions of the relevant parameters	8
2.3	Scaling laws	8
2.3.1	Static scaling laws	9
2.3.2	Dynamical scaling laws	9
2.3.3	Numerical simulations	10
2.4	Treadmilling	11
3	Microrheology	14
3.1	Single bead passive microrheology in a pure solvent	14
3.2	Single bead microrheology in an actin network	15
3.2.1	Complex Elastic Modulus	15
3.2.2	Scaling properties	15
3.2.3	Simulations	16
4	Conclusion	18
A	Langevin equation derivation	19
A.1	Rigid rod segments	19
A.1.1	Hamiltonian	19
A.1.2	Partition function	19
A.1.3	Evaluation of the partition function	20
A.1.4	Path integral expression of the partition function	21
A.2	Continuous persistent chain	21
A.2.1	Equivalence between discrete and continous constraints	21
A.2.2	Continous partition function under constraints	22
A.3	Langevin equation	23
A.3.1	Equation of motion	23
A.3.2	Langevin equation	23
B	Scaling Laws derivations	24
B.1	Worm Like Chain Hamiltonian	24
B.2	Langevin equation	25
B.3	Oseen Tensor	25

Chapter 1

Introduction

General introduction

Cells are complex and active biological objects, comprising many structures and multiple metabolic processes. The metabolic processes convert the chemical energy, generally under the form of Adenine TriPhosphate (ATP), presents in the cell into mechanical work, to perform a wide variety of processes. These biological structures, which comprises membranes, polymeric filaments and molecular machines, enter the broad class of active matter in physics, which describes non-equilibrium processes driven by a continuous energy supply [1].

The **cytoskeleton** is present in most cells, and is a complex network of interlinking filaments and tubules that extend throughout the **cytoplasm**. It contributes to the intracellular transport, cellular mobility, structure and shape of the cell [2]. Filaments of the cytoskeleton belong to three families : **actin filaments**, **microtubules** and **intermediate** filaments, and are the main semi-flexible polymers.

A polymer is a macromolecule, a molecular assembly of many repeated smaller molecules, the monomers. Polymers have a biological origin, but can also be synthetic, and they have a key role in the life of a cell. They have multiple shapes and purposes, from the DNA that encodes the genetic information to the microtubules that drive the division of the cell. Depending on their structure and molecular assembly, polymers present different mechanical and chemical features.

A polymer is said to be **semi-flexible** when its **bending energy** is of the same order as thermal energy [3]. Semi-flexible polymers are characterized by their **persistence length**, the length over which a polymer appears straight in the presence of Brownian forces, which is of the order of their length. If we consider a filament of length L , the persistence length ℓ_p of this filament can be defined as

$$\langle \mathbf{u}(s) \cdot \mathbf{u}(s') \rangle \sim \exp \left[-\frac{|s - s'|}{\ell_p} \right] \quad (1.1)$$

where $\mathbf{u}(s)$ is the local tangent vector of the filament, at the curvilinear coordinate $0 \leq s \leq L$ (see Figure 1.1). If the persistence length is large with respect to $|s - s'|$, the average orientation correlation is close to 1 and the polymer is straight on the length $|s - s'|$. Thus, semi-flexible polymers are an intermediate state between flexible polymers and rigid polymers (rods), with $a \ll \ell_p < L$, a being the fiber diameter. Indeed, **flexible polymers** have very small persistence length with respect to their contour length (e.g. DNA is a flexible polymer with $50nm$ persistence length), and **rods** have an infinite persistence length. The shape of a semi-flexible polymer results from the competition between entropic and bending forces, and at equilibrium this shape fluctuates around a rod-like shape.

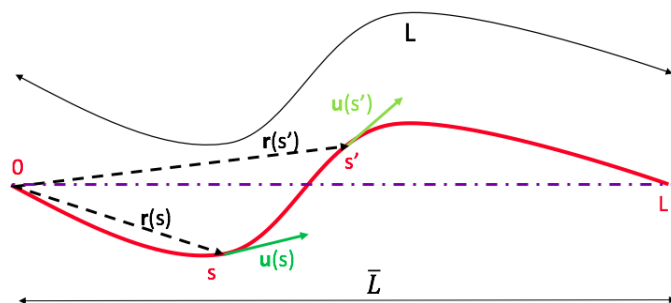


Figure 1.1: Schematic representation of a semi-flexible polymer (red). Its total length (contour length) is L and the **projected length** is \bar{L} , projected on the mean orientation (dashed-dotted line). The positions $\mathbf{r}(s)$, $\mathbf{r}(s')$ and associated tangent vectors $\mathbf{u}(s)$, $\mathbf{u}(s')$ are shown.

Amongst semi-flexible polymers, actin filament is widely spread in eukaryotic cells. Actin is a family of proteins, and is an essential element of the cytoskeleton : it determines the shape of the cell's surface, the cell locomotion, the pinching of the cell into two during mitosis... It is composed of monomers, the **G-actin** (Globular actin), that assemble in presence of a polymerization buffer to form a polar double-helix structure of $a = 5 - 9nm$ diameter, the **F-actin** (Filament actin) [4]. The polar ends are a consequence of the G-actin shape : a **pointed** (-) and a **barbed end** (+). Actin filaments are too thin to be directly seen using optical microscopy, but an observation is still possible using fluorescence techniques and the analysis of their thermal fluctuations leads to measure of their flexural rigidity and persistence length [5]. In the cell, F-actin undergoes fast polymerization and depolymerization, which plays a critical role in cell migration for instance [6]. The filament continuously adds and loses monomers at its ends. However, the barbed end (+) generally has higher concentration of F-actin-ATP and denotes the **growing** (polymerizing) end filament, while the pointed (-) end has higher F-actin-ADP and denotes the **shrinking** (depolymerizing) end filament. Adjusting the rates of polymerization / depolymerization using chemical enhancers may induce, when the two rates are equal, a steady-state for the length of the filament. This is an out-of-equilibrium but stationary process for the filament, the so-called **treadmilling** filament.

Semi-flexible polymer networks, such as the cytoskeleton, are complex structures, with many components in living cells : biopolymers, cross-linkers, molecular motors, etc. Experimentally, *in-vitro* biopolymer networks are reconstituted gels containing the desired ingredients under well-controlled conditions, in order to study simplified systems. On a macroscopic scale, semi-flexible polymer networks exhibit viscoelastic properties, due to the entangled nature of such networks.

State of the art

Single polymer

The study of polymers is an old problem in physics and semi-flexible polymer physics started with a simple model : the Worm Like Chain (WLC) model [7]. From this model, many equilibrium effects were investigated on theoretically : the force-extension relation of a filament [8], dynamic light scattering of entangled networks [9, 10], the static [11] and dynamic thermal fluctuations with power-law behaviors [12, 13], as well as experimental results on the persistence length of actin [5, 14] for instance. Simulations of theoretical models were also proposed to support experimental results on the dynamics of a semi-flexible polymer [15, 16]. However, all these effects have been studied at equilibrium, under very specific conditions : in particular polymerization and depolymerization have not been considered since it is still experimentally hard to control the disassembly rate of fibers, though it exists and is of critical importance in multiple phenomena such as cell mobility. The effect of treadmilling on the dynamics of a semi-flexible polymer remains uncharacterized.

Microrheology

Polymer solutions are a mix of many polymers in a solvent (usually water), than can entangle and interact via steric interactions. These solutions exhibit very interesting optical, dielectric and mechanical features [17] : from the mechanical point of view, such solutions are an intermediate between a solid and liquid state, since the polymers may move inside the network they form and modify its structure. Therefore, polymer solutions exhibit both viscous and elastic properties. Actin networks are such solutions, and their properties are still studied experimentally, for instance the effects of cross linkers [18] in this medium or dilute and crystalline solutions [19]. The typical distance between filaments in an actin network, the **mesh size**, is $\xi \sim a/\sqrt{\phi}$ with a the diameter of a fiber and ϕ the polymer volume fraction [3, 18].

Microrheology consists in the measure of the rheological properties, e.g. the viscoelasticity, of a medium. In our case, we consider entangled actin networks, and we use beads embedded inside the medium to measure its rheological properties. The size of the beads is chosen such that the bead is large enough to be trapped by the surrounding network, that forms a cage, and small enough to be sensitive to the forces applied by the fluctuating fibers. Two types of microrheology can be distinguished : passive and active microrheology. Active microrheology consists in applying an external force (using optical or magnetic tweezers) on a bead and observing the response of the medium, but we will not discuss about it here. Instead, we focus on passive microrheology, which is the measure of the mean square displacement of a bead in the medium, related to its bulk properties. Passive microrheology can also be splitted into 1- and 2-particle microrheology [20, 21]. The second one, which is again not discussed here, tries to cancel the local disturbance of the bead on the medium by measuring the correlations between two beads separated by a distance larger than the local disturbance.

One of the fundamental properties of such networks is the **shear modulus**, G , that describes the viscoelastic properties of the materials and their mechanical response under a shear stress. Shear modulus is a macroscopic property, due to the structure of the network : entanglement of polymers, crosslinkers, steric interactions, etc. and to the thermal fluctuations of the filaments. The shear modulus shows a frequency dependence, such as plateau moduli

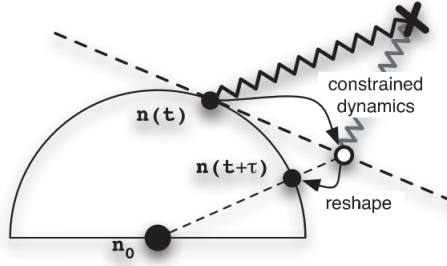


Figure 1.2: Dynamics with constraints : one step of the algorithm is shown. The point $n(t)$ is initially at a distance $r = |n(t) - n_0|$ from n_0 . This constraint defines a sphere of radius r and center n_0 . Its motion is calculated from Eq. (1.2) in the tangent plane to the sphere, and the constraint is exactly respected by a projection of the point onto the sphere, to give the new position $n(t + \tau)$. From [29].

[22, 23, 24, 25, 26] or power-law behavior [21]. The shear modulus of actin networks has been experimentally measured with 1- and 2-particle microrheology [27] and active microrheology [28].

However, no previous study of treadmilling filament networks has been carried out, either experimentally or numerically.

Cytosim

Biological polymer networks are complex systems, hard to understand from a direct theoretical point of view. Simulations are therefore needed as a tool to test hypothesis and compare experiments to the theory. For instance, the actin cytoskeleton includes a lot of different elements and active processes, making the analytical treatment sometimes intractable. Cytosim is a C++ based software, developed by F. Nedelec and others [29], to study the stochastic dynamics of an ensemble of various agents such as fibers, molecular motors or other objects. Cytosim generates discrete objects mimicking real cytoskeletal elements, described by their positions in a pre-defined space. Each object can be defined with a very large number of tunable parameters, written in a configuration file. The coordinates of each object are stored in a $N.d$ vector (d the dimension, N the number of points of the object). At the molecular scale, the equation of motion of an object is given by the (discrete) overdamped Langevin equation ([29, 30]) :

$$d\mathbf{x} = \underline{\underline{\mu}}\mathbf{F}(\mathbf{x}, t) + d\xi(t) \quad (1.2)$$

with $\underline{\underline{\mu}}$ a mobility matrix, \mathbf{F} the vector of forces (size $N.d$), $d\xi(t)$ a Brownian force (size $N.d$) with zero mean and unitary variance. For some objects, such as fibers or beads, distances must be conserved, so an additional constraint must be included. The dynamics of the Langevin equation is solved with an implicit integration scheme that uses an Euler backward equation that avoids the appearance of spurious oscillations in the system (see [29]). For a unique point, its Langevin equation is solved in a plane defined as the tangent subspace to the constraints manifold : this is the so-called *constrained dynamics*. The constraint is then included and the positions are projected in such a way that the constraint is respected exactly (see Fig 1.2).

To simulate microrheology experiments, we will use mostly two objects in Cytosim, fibers and beads, to generate a network of entangled fibers surrounding a bead, and we will track the position of the bead center. Fibers are modeled as a collection of points, representing an infinitely thin filament, composed of inextensible segments (rod-like) linking two successive points of the fiber. The length of each segment is calculated at each step and the number of segments is adjusted as a function of the total length L in order to respect the segmentation constraint. The bending stiffness of the filament is calculated as a bloc-matrix and included in the Langevin equation. For simplicity, we will consider the 2D case for single filament (as most papers do). The persistence length of the chain is arbitrarily fixed via the bending stiffness of the chain in a configuration file, as well as other parameters of the simulation (temperature, viscosity of the solvent, time step, total simulation time, etc.). Spheres, such as the microbeads used in microrheology experiments or as approximation of the nucleus of a cell, can also be included in Cytosim. The sphere moves as a rigid body in viscous fluid. Steric interactions are implemented as a Hook's law, and the rigidity of the spring is given as a tunable parameter.

We want to use Cytosim as a practical tool to perform *in silico* microrheology experiments.

Objectives and goals

The main purpose of this project is to study microrheology of actin networks, first by reproducing *in silico* microrheology experiments, then including the treadmilling of polymers in the network and quantifying its effects. The rheology

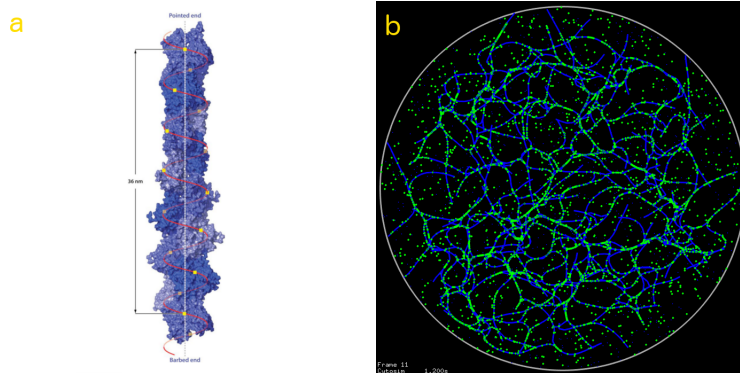


Figure 1.3: (a) F-actin helical structure, with pointed (top) and barbed (bottom) ends, from [2] ; (b) Cytosim is able to do many different simulations : here is a 2D contractile actin network (blue filaments) with molecular motors (green points) and cross linkers (blue points).

of entangled networks is dictated by the diameter of the exclusion tube, itself determined by the amplitude of fluctuations of the filaments [22, 23, 24]. Therefore we want to start our study by considering a single "classical" semi-flexible polymer and look at its fluctuations at equilibrium, then introduce the polymerization and depolymerization in order to quantify their effects on the spectrum of fluctuations of a single semi-flexible polymer and predict the behavior of turnover entangled networks. At the same time, we want to investigate the microrheology of actin networks, first considering "classical" semi-flexible polymer network, then introducing the polymerization of the fibers in the network to make predictions for the microrheology of actin networks.

Plan

This report is splitted in three parts, the two firsts being independent. In the first part we will first look at the dynamics of a single semi-flexible polymer, deriving its partition function and the Langevin equation for the position of the filament. From the Langevin framework, we will focus on the thermal fluctuation properties of the filament. Then, we will present numerical results and hypothesis on the treadmilling semi-flexible polymer. In a second part, we will study the microrheology of semi-flexible polymer (actin-like) networks, using the 1-particle passive microrheology technique. Eventually, we will discuss our results and present what may be the future steps of this project.

Chapter 2

Single filament study

In this chapter, we will focus on the properties of a single polymer semi-flexible filament : its equilibrium dynamical fluctuations and preliminary results on a treadmilling polymer.

2.1 Equilibrium properties

2.1.1 Discrete chain model

A polymer consists in a chain of small molecular elements, the monomers, of given length that we will denote ℓ . In our study, the monomer length is not necessarily the real size of a single monomer, but a coarse-grained length, typically the smallest value that we can observe. This length will play the role of a cut-off, and in simulations, it will corresponds to the arbitrary spatial discretization of the polymer.

Let us consider a chain of N monomers, each denoted as M_i ($i = 1, \dots, N$) and of mass m . The positions of the two ends of a monomers are denoted as \mathbf{r}_{i-1} (first end) and \mathbf{r}_i (last end), where \mathbf{r}_i is the position with respect to the origin. We define \mathbf{r}_0 to be at the origin of our coordinates system, so that the polymer has no translational degrees of freedom (translationally invariant model).

Instead of considering the positions \mathbf{r}_i , we introduce another vector, \mathbf{R}_i , describing the orientation of the segment linking the ends of monomers i and $i - 1$, such that

$$\forall i = 1, \dots, N, \mathbf{R}_i = \mathbf{r}_i - \mathbf{r}_{i-1} \quad (2.1)$$

Within these conditions, we can write the Hamiltonian of this chain as a kinetic energy for each monomer (except the monomer $i = 0$ since it is fixed) plus a harmonic potential that describes the interaction between two monomers

$$\mathcal{H} = \sum_{i=1}^N \frac{\mathbf{p}_i^2}{2m} + \frac{v_0}{2} \sum_{i=1}^N (|\mathbf{R}_i| - \ell)^2 \quad (2.2)$$

with v_0 a *stiffness constant*, homogenous to a force per unit length. This harmonic potential is a coarse-grained quantity, where ℓ is the *equilibrium length* of a monomer $\langle |\mathbf{R}_i| \rangle = \ell$. In the limit $v_0 \rightarrow \infty$, the elastic force deriving from the harmonic potential becomes infinite, and our chain becomes inextensible and rigid.

In semi-flexible polymer physics, a key parameter is the bending stiffness of the chain, that characterizes its inflexibility. We introduce it as a mean field approximation

$$\forall i = 1, \dots, N, \langle \mathbf{R}_i \cdot \mathbf{R}_{i+1} \rangle = \ell^2 \cdot \sigma \quad (2.3)$$

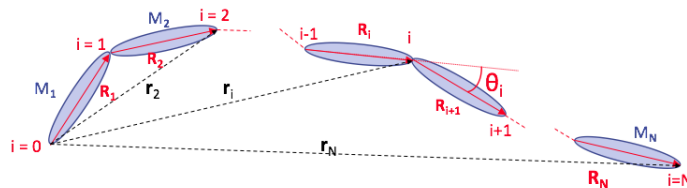


Figure 2.1: The discrete polymer model, with N monomers. Coarse grained monomers are labeled as M_i and have rod-like shape (blue ellipses). Monomer M_i has ends' positions \mathbf{r}_{i-1} and \mathbf{r}_i with respect to the origin $\mathbf{r}_0 \equiv \mathbf{0}$. The orientation \mathbf{R}_i of monomer M_i is defined as Eq (2.1). The angle $\cos(\theta_i) = \mathbf{R}_i \cdot \mathbf{R}_{i+1} / \ell^2$ is represented.

where $\sigma = \langle \cos(\theta_i) \rangle$ is the **stiffness parameter**, such that in the limit $v_0 \rightarrow \infty$, the chain becomes locally rod-like, and the angle between two consecutive segments \mathbf{R}_i and \mathbf{R}_{i+1} becomes flat ($\theta_i = 0$) therefore

$$\lim_{v_0 \rightarrow \infty} \sigma = \lim_{\theta_i \rightarrow 0} \langle \cos(\theta_i) \rangle = 1 \quad (2.4)$$

2.1.2 Partition function

At equilibrium, we can write the discrete partition function using the **Maximum Entropy Principle** (see [31], Chapter 12.) as

$$\mathcal{Z} = \int d^{3N} R \prod_{i=1}^N \delta(|\mathbf{R}_i| - \ell) \exp \left[-\frac{\mu}{2} \sum_{i=1}^{N-1} (\mathbf{R}_{i+1} - \mathbf{R}_i)^2 \right] \quad (2.5)$$

where μ is a Lagrange multiplier for the constraint Eq. (2.3). The derivation of Eq. (2.5) is given in Appendix A.1.

It is customary to use a continuous representation of the chain, so that the set of individual monomers positions $\{\mathbf{r}_i\}$ becomes a continuous function $\mathbf{r}(s)$ where $s \in [0, L]$ is the arclength along the filament. In this representation, the partition function and the Hamiltonian are no more constants, but functionals. This continuum limit is obtained using the limits

$$N \rightarrow \infty \quad \ell \rightarrow 0 \quad N\ell = L \quad \sigma \rightarrow 1 \quad (2.6)$$

so that we end up with the functional partition function (see derivation in Appendix A.1.4)

$$\mathcal{Z} = \int \mathcal{D}^3 R \exp \left[-\frac{\kappa}{2} \int_0^L ds \left(\frac{\partial^2 \mathbf{r}(s)}{\partial s^2} \right)^2 \right] \quad (2.7)$$

$$\mathcal{D}^3 R = \lim_{\substack{\ell \rightarrow 0 \\ N \rightarrow \infty}} d^{3N} R \prod_{i=1}^N \delta(|\mathbf{R}_i| - \ell) \quad (2.8)$$

We identify the exponent in the exponential as the - functional - Hamiltonian for a semi-flexible polymer with bending modulus κ , as usually defined. The bending modulus is given by the relation (A.16), and from it, we can define the persistence length, as

$$\kappa \equiv k_B T \ell_p \quad (2.9)$$

where $k_B T$ is the thermal energy. This is equivalent to definition (1.1) of ℓ_p for $|s - s'| \rightarrow 0$. The persistence length is the characteristic length over which the filament "looses" its spatial correlations, ie: the length over which it cannot be considered as a rod. The typical persistence length for actin polymers is around 9 – 10nm [14] at 37°C, corresponding to a bending modulus of $0.04pN \cdot \mu m^2$.

Inside the chain, there is a tension that contributes to the energy, by propagating strain along the chain. In our expression of (2.7), this is hidden in the integrand (see Eq. (2.8)), which is equivalent to the discrete expression of Eq. (2.5), with the delta-function that stands for the inextensibility of the segments. Moreover, the total length of the chain is fixed, and is equal to L , and that is another constraint. Finally, an additional constraint arises from the mean-field approximation we made in Eq. (2.3). All these constraints are given in Eq. (A.17) - (A.22). Using the discrete constraints to introduce Lagrange multipliers τ_0 and $\tau(s, t)$ and taking a continuum limit (cf Appendix A.2.2), we end up with the final partition function

$$\mathcal{Z} = \int \mathcal{D}^3 R \exp \left\{ -\int_0^L ds \tau(s, t) \left(\frac{\partial \mathbf{r}(s)}{\partial s} \right)^2 - \tau_0 \left[\left(\frac{\partial \mathbf{r}(0)}{\partial s} \right)^2 + \left(\frac{\partial \mathbf{r}(L)}{\partial s} \right)^2 \right] - \frac{\kappa}{2} \int_0^L ds \left(\frac{\partial^2 \mathbf{r}(s)}{\partial s^2} \right)^2 \right\} \quad (2.10)$$

2.1.3 Langevin equation

We want now to consider the motion of the chain in a solvent with a viscosity ζ_s and at temperature T . Note that we must now take $\mathbf{r}(s)$ as a time dependent function. We first compute the Lagrangian associated with the Hamiltonian identified in the exponent of (2.10) and we consider also the kinetics of the chain. Using the Euler-Lagrange theorem - valid since we are at equilibrium - we can find the equation of motion of the chain as (see Part B.2)

$$\rho \partial_t^2 \mathbf{r} - 2 (\partial_s \tau \partial_s \mathbf{r} + \tau(s, t) \partial_s^2 \mathbf{r}) + \kappa \partial_s^4 \mathbf{r} = 0 \quad (2.11)$$

To this equation of motion, we add the viscous force $-\underline{\zeta} \partial_t \mathbf{r}(s, t)$, where $\underline{\zeta} = \zeta_{\parallel} \partial_s \mathbf{r} \otimes \partial_s \mathbf{r} + \zeta_{\perp} [\underline{\mathbf{I}} - \partial_s \mathbf{r} \otimes \partial_s \mathbf{r}]$ is a friction tensor, since the longitudinal friction, ζ_{\parallel} , is different from the transverse friction ζ_{\perp} . Transverse and

longitudinal frictions are related to the solvent viscosity ζ_s via $\zeta_{\parallel} = \zeta_{\perp}/2 = 2\pi\zeta_s$ [10]. We also add a brownian force $\boldsymbol{\xi}(s, t)$, defined such that

$$\langle \boldsymbol{\xi}(s, t) \rangle = \mathbf{0} \quad (2.12)$$

$$\langle \xi_i(s, t) \xi_j(s', t') \rangle = 2\zeta_{i,j} k_B T \delta_{i,j} \delta(s - s') \delta(t - t') \quad (2.13)$$

where i, j designate the components of the vector, $\delta_{i,j}$ is the Kronecker delta and $\delta(x)$ is the Dirac function. We consider the overdamped regime, so the inertial term $\rho \partial_t^2 \mathbf{r}(s, t)$ is negligible, and the Langevin equation for a semi-flexible polymer with bending modulus κ in a solvent of viscosity ζ_s at temperature T is

$$\zeta \partial_t \mathbf{r}(s, t) + \kappa \partial_s^4 \mathbf{r}(s, t) - 2\partial_s \tau(s, t) \partial_s \mathbf{r} - 2\tau(s, t) \partial_s^2 \mathbf{r}(s, t) = \boldsymbol{\xi}(s, t) \quad (2.14)$$

In absence of tension terms, the above equation resembles a diffusion equation, but the second order spatial derivative has been replaced by a fourth order spatial derivative. This may lead the amplitude of fluctuations to follow an anomalous power-law dynamics, as we shall see.

2.2 Definitions of the relevant parameters

In order to properly define the relevant parameters, we follow the parametrization of [15]. Since we consider chains such that $L \lesssim \ell_p$, we can define an average orientation at time t , given by $\hat{\mathbf{u}}_0(t) = \frac{\int_0^L ds \hat{\mathbf{u}}(s, t)}{|\int_0^L ds \hat{\mathbf{u}}(s, t)|} = \frac{\mathbf{r}(L, t) - \mathbf{r}(0, t)}{|\mathbf{r}(L, t) - \mathbf{r}(0, t)|} = \hat{\mathbf{R}}(t)$ which is nothing but the normalized end-to-end vector $\mathbf{R}(t)$ of the filament. The local orientation at point s may be written

$$\hat{\mathbf{u}}(s, t) = \hat{\mathbf{u}}_0(t) + \delta \mathbf{u}(s, t) \quad (2.15)$$

where $\delta \mathbf{u}$ is a local perturbation, that can be written in a orthonormal basis $\{\hat{\mathbf{e}}_x(t), \hat{\mathbf{e}}_y(t), \hat{\mathbf{u}}_0(t)\}$ (see Fig. ??) as

$$\delta \mathbf{u}(s, t) = u_x(s, t) \hat{\mathbf{e}}_x(t) + u_y(s, t) \hat{\mathbf{e}}_y(t) + u_z(s, t) \hat{\mathbf{u}}_0(t) \quad (2.16)$$

The local orientation $\hat{\mathbf{u}}(s, t)$ and the filament position $\mathbf{r}(s, t)$ are related as $\hat{\mathbf{u}}(s, t) = \partial_s \mathbf{r}(s, t)$, so that the filament position also reads, using Eq. (2.15)

$$\mathbf{r}(s, t) = \mathbf{r}(0, t) + [s + r_z(s, t)] \hat{\mathbf{u}}_0(t) + r_x(s, t) \hat{\mathbf{e}}_x(t) + r_y(s, t) \hat{\mathbf{e}}_y(t) \quad (2.17)$$

where $\mathbf{r}(0, t)$ is the position of one of the ends of the filament. Before, we fixed it to be the origin, but in the case where the filament is treadmilling, we have to release this constraint. The coordinates (x, y) will thus refer to the **transverse** direction(s), so that $\mathbf{r}_{\perp}(s, t) = (u_x(t), u_y(t))$, and the coordinate z will refer to the **longitudinal** direction, thus $r_{\parallel}(s, t) = s + r_z(s, t)$. In 2-d, there is only one transverse direction. The position of the center of mass, denoted as $\mathbf{r}_0(t)$ is given by

$$\mathbf{r}_0(t) = \frac{1}{L} \int_0^L \mathbf{r}(s, t) ds \quad (2.18)$$

The projected length at time t , $\bar{L}(t)$, is defined as [13]

$$L = \int_0^{\bar{L}(t)} ds \sqrt{1 + (\partial_s \mathbf{r}_{\perp}(s, t))^2} \quad (2.19)$$

and the mean projected length is [13]

$$\langle \bar{L}(t) \rangle \simeq L \left(1 - \frac{1}{6} \frac{L}{\ell_p} \right) \quad (2.20)$$

2.3 Scaling laws

We want now to calculate the main asymptotic behaviors of a semi-flexible filament, having either temporal or spatial dependency. We will first consider the spatial static scaling properties at equilibrium of the polymer chain, then the dynamical scaling properties coming from the Langevin dynamics of the chain.

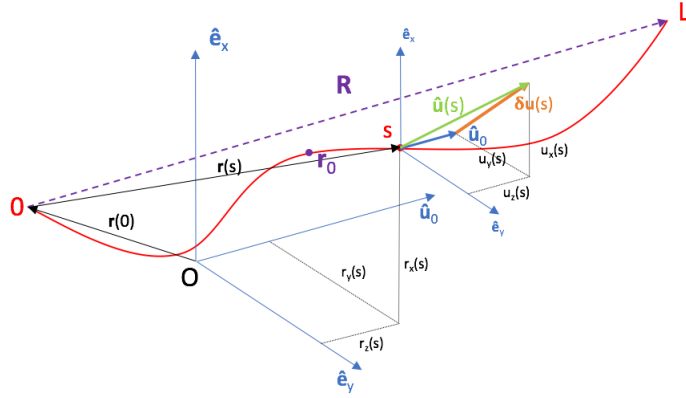


Figure 2.2: The 3d-local frame $\{\hat{e}_x, \hat{e}_y, \hat{u}_0\}$ for a filament of length L . Time is omitted for clarity. The local orientation $\hat{u}(s)$ is represented as decomposition Eq. (2.15), the filament position $\mathbf{r}(s)$ as Eq. (2.17). The first end of filament is denoted $\mathbf{r}(0)$, \mathbf{R} is the end-to-end vector and \mathbf{r}_0 the center of mass.

2.3.1 Static scaling laws

From the equation (2.7), we can write the so called Worm Like Chain Hamiltonian

$$\mathcal{H}[\mathbf{r}] = \frac{\kappa}{2} \int_0^L ds \left(\frac{\partial^2 \mathbf{r}(s)}{\partial s^2} \right)^2 \quad (2.21)$$

for a continuous chain of length L , with arclength s , and with bending modulus κ . Using the Fourier representation of $\mathbf{r}(s)$ as $\mathbf{r}(s) = \int \frac{dq}{2\pi} \mathbf{r}_q e^{iqs} = \frac{1}{L} \sum_q \mathbf{r}_q e^{iqs}$ and inserting it into the Hamiltonian, we find

$$\mathcal{H} = \frac{\kappa}{2} \int \frac{dq}{2\pi} q^4 |\mathbf{r}_q|^2 \quad (2.22)$$

Note that we do not specify the interval of integration for the Fourier integral, because depending on the characteristic lengths, the interval may change (and it changes from one article to another in literature). However, we have two characteristics lengths in our system : the total length L of the polymer (roughly equal to the projected length \bar{L} at first order approximation), and the segmentation of the polymer in the simulations, which is a coarse-grained monomer length, that we will call b . Therefore, even if we do not specify here, we assume that the interval of integration is $[\frac{2\pi}{L}, \frac{2\pi}{b}]$, where $b \ll 1 \ll L$. Applying equipartition theorem on this Hamiltonian, $\langle \mathcal{H} \rangle = N \frac{k_B T}{2}$, we have

$$\langle |\mathbf{r}_q|^2 \rangle = \frac{k_B T L}{\kappa q^4} \quad (2.23)$$

which leads to the following static scaling law, that was first demonstrated by [11] :

$$\langle \delta \mathbf{r}^2(\ell) \rangle \sim \frac{\ell^3}{\ell_p} \quad (2.24)$$

This scaling tells us that if we consider the tube formed by the transverse fluctuations of the filament, the exclusion tube, its typical diameter tube scales as $L^{3/2}$.

2.3.2 Dynamical scaling laws

Up until now, we have only described a chain at equilibrium with no external forces. But as seen in Section 2.1.3, we can include hydrodynamics to our equations, resulting in the Langevin equation (2.14) and makes $\mathbf{r}(s)$ time dependent. Nevertheless, this Langevin equation being rather complicated to treat, we simplify our study using scaling arguments on a simpler Langevin equation with vanishing tension terms, which is a good approximation for transverse dynamics. Scaling arguments, give however the correct scaling laws, up to logarithmic corrections. An exact calculation of the scalings would lead to renormalization group calculation [10], which goes beyond the scope of this report. Using the spatial and temporal Fourier transformation, we can find the equivalent (simplified) Langevin equation for the transverse coordinates [12, 13]

$$i\omega \zeta_{\perp} \tilde{\mathbf{r}}_{\perp}(q, \omega) = -\kappa q^4 \tilde{\mathbf{r}}_{\perp}(q, \omega) + \tilde{\boldsymbol{\xi}}_{\perp}(q, \omega) \quad (2.25)$$

Using the characteristic time extracted from this Langevin Equation, $\tau \sim \frac{\zeta_{\perp}}{\kappa} \ell^4$, and the relation (2.24), we find in the asymptotic limit $\frac{\zeta_{\perp} b^4}{\kappa} \ll t \ll \frac{\zeta_{\perp} L^4}{\kappa}$ the amplitude of fluctuations to be (see Appendix B.1)

$$\langle \delta r_{\perp}^2(t) \rangle \sim \frac{k_B T}{\zeta_{\perp}^{3/4} \kappa^{1/4}} t^{3/4} \sim t^{3/4} \quad (2.26)$$

This behavior has been experimentally verified [9, 32]. These calculations can be conducted more rigorously (see Appendix B.3, [13]), considering instead of a local homogenous friction ζ_{\perp} the Oseen Tensor and neglecting logarithmic terms, and it gives the following expression for the temporal MSD

$$\langle \delta r_{\perp}^2(t) \rangle = \frac{4k_B T}{\pi \kappa} \int_{\pi/L}^{\pi/b} \frac{dq}{q^4} \left(1 - e^{-\omega(q)t}\right) \quad (2.27)$$

where $\omega(q) \simeq \frac{\kappa k^4}{\zeta_{\perp}} \ln\left(\frac{1}{qb}\right)$. However, above this range of time, the MSD saturates to the equilibrium value

$$\langle \delta r_{\perp}^2 \rangle = \frac{2}{45} \frac{k_B T}{\kappa} L^3 \quad (2.28)$$

where we have used the explicit summation over the modes for Eq. (2.27) to get the prefactor. We note that we recover the static scaling in L^3/ℓ_p , already calculated in Eq. (2.24).

For longer times, the longitudinal fluctuations will follow the same scaling law as the transverse fluctuations : the static longitudinal fluctuations scale as $\langle \delta r_{\parallel}^2 \rangle \sim \ell_1^4/\ell_p^2$, and since each section of length ℓ_1 is independent, it contributes to the mean square longitudinal fluctuations with the static longitudinal fluctuations scaling. Therefore, for a filament of total length L , the L/ℓ_1 sections of the filament contribute with that static longitudinal scaling, so that

$$\langle \delta r_{\parallel}^2(t) \rangle \sim \frac{L}{\ell_1} \cdot \frac{\ell_1^4}{\ell_p^2} = \frac{L t^{3/4}}{\ell_p^{5/4}} \sim t^{3/4} \quad (2.29)$$

Another scaling law was also extracted for longitudinal fluctuations on shorter times, using scaling arguments and the fluctuation dissipation theorem [12], or renormalization group calculations [10] or studying the dynamics of connected rods [15]. If we consider local and global inextensibility constraints carefully, we must use Eq. (2.14), but it is rather complicated, so we use a scaling argument. The inextensibility of the segments introduces a tension in the chain, and this tension propagates longitudinal fluctuations on short time, in competition with the local viscous longitudinal drag. This gives us the amplitude of longitudinal fluctuations at short times as follow [12] : on one hand, due to the friction, the entire filament cannot instantaneously moves, but only a length ℓ_2 can, with speed $v_{\parallel} \sim \delta r_{\parallel}/t$, due to a force $f_{\parallel} \sim v_{\parallel} \ell_2$, so $\delta r_{\parallel} \sim \frac{t f_{\parallel}}{\ell_2}$. On the other hand, at equilibrium, the fluctuation dissipation theorem (FDT) gives, using Eq. (2.29), $\delta r_{\parallel} \sim f_{\parallel} \langle \delta r_{\parallel}^2 \rangle \sim f_{\parallel} \frac{\ell_2 t^{3/4}}{\ell_p^{5/4}}$. Thus, $\ell_2 \sim t^{1/8} \ell_p^{5/8}$, and injecting it inside Eq. (2.29) for $L = \ell_2$, we find

$$\langle \delta r_{\parallel}^2(t) \rangle \sim t^{7/8} / \ell_p^{5/8} \sim t^{7/8} \quad (2.30)$$

We give the full expression of $\langle \delta r_{\parallel}^2(t) \rangle$ containing all terms at Eq. (B.7).

2.3.3 Numerical simulations

The predefined contour length L and the segmentation b of the filament are changed so that the number of segments is constant, and allow the simulations to cover different time scales : from them we can define two characteristic times

$$t_{\min} = 4\pi \frac{\zeta_s b^4}{\kappa} \quad t_{\max} = 4\pi \frac{\zeta_s L^4}{\kappa} \quad (2.31)$$

used to determine the time step and the duration of the simulation. The relaxation times of the largest modes are of the order of t_{\max} , so we (arbitrarily) set the time for a filament to be considered as equilibrated as $t_{eq} = 100 \cdot t_{\max}$, while the time step is defined as $t_{step} = 10^{-2} t_{\min}$, so that we cover 5 temporal decades. Typical relaxation times for a filament of the order of $10 \mu m$ are several tens of seconds. For each configuration of parameters with given fixed length and segmentation, we generate first 50 equilibrated configurations, then we run 100 simulations for each equilibrated configuration. Our simulation time is limited to $10^5 t_{step}$, in order to avoid rotational diffusion of the filament at long times that would break our scaling laws [12] because of the distortion of the ellipsoidal cloud into a "croissant"-like cloud. For a filament with length $10 \mu m$, the typical rotational time is of the order of [15] $\tau_{rot} \sim \frac{1}{2D_r} = \frac{\zeta_s L^3}{6k_B T} \simeq 1s$ (same viscosity and temperature) while our total simulation time is of the order of $t_{simu} \simeq 10^{-2} s$.

We extract the transverse and longitudinal amplitudes of fluctuations $\langle \delta r_{\perp, \parallel}^2(t) \rangle$ for the two ends of the filament by calculating the moments of the 2d-clouds in their local basis (see Fig. 2.3). We use diagonalized covariant matrices to determine this basis, the largest eigenvalue (resp. smallest) of the covariant matrix corresponding to the transverse (resp. longitudinal) direction. For a given time step of a configuration, a 2d-cloud is composed of the positions of a

given end for the 100 simulations. The amplitudes of fluctuations in each direction correspond to the MSD along the local cloud-axis. The MSD of each simulation is computed using the Fast Fourier Transform method (see Part 3.1 and [33]). MSD are first averaged on all simulations and then on all configurations with the same parameters. In order to illustrate the power-law scalings, we "glue back together" the transverse and longitudinal amplitudes of fluctuations of different lengths and segmentation, covering overlapping time decades (Fig. ??). As predicted in [12], [13], and demonstrated above, we recover two scaling laws : for transverse amplitudes, the $t^{3/4}$ scaling is found at large times ; for longitudinal fluctuations, the $t^{3/4}$ is found at large times, and $t^{7/8}$ is found at small times.

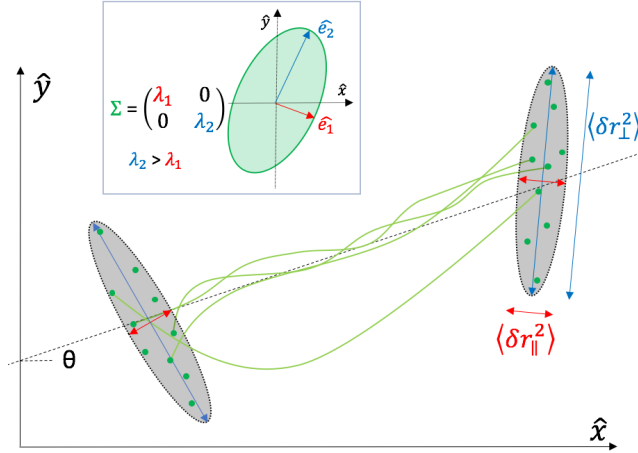


Figure 2.3: Schematic representation of the clouds of points at a given time step t in 2D. The clouds are the collection of ends' positions (green dots) of the fibers (green fibers) and form ellipses (grey ellipses). Directions of the ellipses are calculated by diagonalizing the covariant matrices for both ends : the largest (resp. smallest) eigenvalue has eigenvector corresponding to the transversal (resp. longitudinal) fluctuations (blue direction, resp. red direction). The eigenvectors give the local orientation of the cloud. θ is the angle of the mean orientation of the fibers (black dotted line) with one of the vectors of the absolute frame $\{\hat{x}, \hat{y}\}$. Inset : the eigenvectors $\hat{e}_{1,2}$ with associated eigenvalues $\lambda_{1,2}$ of a diagonalized covariant matrix σ of a generic cloud.

2.4 Treadmilling

Now that we have characterized the equilibrium amplitudes of fluctuations of a semi-flexible polymer, we can ask ourselves : what is the effect of polymerization and depolymerization on the fluctuations ? We consider a simple model, and we will try to derive some equations to describe the dynamics. We consider a polymer of length L , at equilibrium, following the same equations we established before, and we add polymerization (resp. depolymerization) at the (+) (resp. (-)) end, in such a way that the rates of polymerization k_p and depolymerization k_d are equal. This is an important hypothesis, that allow us to consider a stationary state where the total length of the polymer remains constant : the polymer is said to **treadmill**. Moreover, we assume that the polymerization and depolymerization are continuous processes in time. From the (de)polymerization rates, we can define the treadmilling speed $v_p = k_p \cdot b = k_d \cdot b$ where b is the monomer length.

From a kinematic point of view - without thermal motion, and neglecting bending and tension - the equations of motion for the position $\mathbf{r}(s, t)$ and orientation $\hat{\mathbf{u}}(s, t)$ of the polymer is given by

$$\underline{\zeta} \partial_t \mathbf{r}(s, t) = v_p \underline{\zeta} \partial_s \mathbf{r}(s, t) = v_p \underline{\zeta} \hat{\mathbf{u}} \quad (2.32)$$

$$\zeta_u \partial_t \hat{\mathbf{u}}(s, t) = v_p \zeta_u \partial_s \hat{\mathbf{u}}(s, t) = v_p \zeta_u \partial_s^2 \mathbf{r} \quad (2.33)$$

with $\hat{\mathbf{u}}(s, t)$ is the local tangent vector, defined as Eq. (2.15), and we keep the translational local friction tensor, with $\zeta_{\perp} \sim 2\zeta_{\parallel} \sim \frac{\zeta_s}{\ln(\ell/a)}$ and we introduce $\zeta_u \sim \frac{\zeta_s \ell^2}{\ln(\ell/a)}$ a (rescaled) rotational friction coefficient [34]. This describes a polymer with a "snake-like" motion, as we can see on Fig. 2.5 with changing orientation. It may seem that the polymer is subjected to an external force "pulling" it in a random direction, but the process we have here is different : the polymer removes monomers at one end and adds monomers at its other end. Therefore, our previous Langevin equation (2.14) for the position $\mathbf{r}(s, t)$, is not valid anymore, and we have to adopt another set of equations to describe the motion of the treadmilling polymer, using the equations (see Eqs (12, 13) of [15])

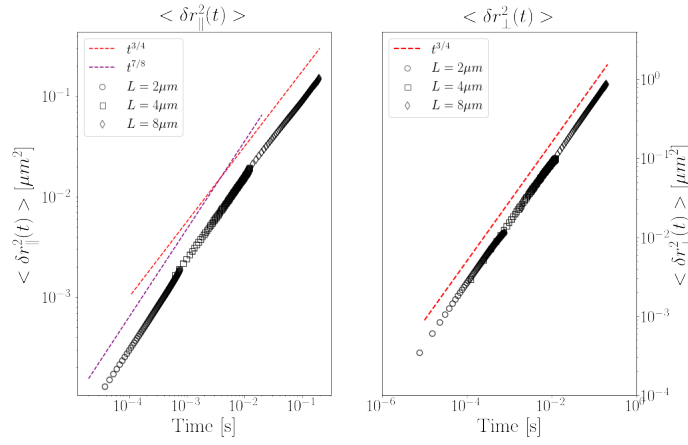


Figure 2.4: Transverse (\perp) and longitudinal (\parallel) amplitude of fluctuations of a semi-flexible polymer as a function of time for different lengths ($L = 2, 4, 8\mu\text{m}$) at constant segmentation ($N = 50$ segments). Transversal fluctuations scales as $\langle \delta r_{\perp}^2(t) \rangle \sim t^{3/4}$ while longitudinal fluctuations scale as $\langle \delta r_{\parallel}^2(t) \rangle \sim t^{7/8}$ at small times then $\langle \delta r_{\parallel}^2(t) \rangle \sim t^{3/4}$ at large times. Dashed lines represent the different power-laws.

$$\zeta_u \partial_t \hat{\mathbf{u}}(s, t) = (\underline{\mathbf{I}} - \hat{\mathbf{u}}(s, t) \otimes \hat{\mathbf{u}}(s, t)) \cdot [\chi_u(s, t) + \xi_u(s, t)] \quad (2.34)$$

$$\underline{\zeta} \partial_t \mathbf{r}(s, t) = \partial_s \chi(s, t) + \xi(s, t) \quad (2.35)$$

$$\chi(s, t) = -\kappa \partial_s^3 \mathbf{r}(s, t) + \tau(s, t) \partial_s \mathbf{r}(s, t) \quad (2.36)$$

with $\xi_u(s, t) \sim \ell \cdot \xi(s, t)$ random force with zero mean and $\langle \xi_{u,i}(s, t) \xi_{u,j}(s, t') \rangle = 2k_B T b \zeta_u \delta_{i,j} \delta(t - t') \delta(s - s')$, and $\partial_s \chi$ is a force term that includes both bending and tension forces.

From those equations we can extract the average properties, i.e : the position of the center of mass $\mathbf{r}_0(t)$ and the mean orientation $\hat{\mathbf{u}}_0(t)$, as defined in 2.2, and they follow the Langevin equations (Eqs (34, 35) of [15])

$$\zeta_u \partial_t \hat{\mathbf{u}}_0(t) = (\underline{\mathbf{I}} - \hat{\mathbf{u}}_0(t) \otimes \hat{\mathbf{u}}_0(t)) \cdot \xi_{u,0}(t) \quad (2.37)$$

$$\underline{\zeta} \partial_t \mathbf{r}_0(t) = \xi_0(t) \quad (2.38)$$

where $\xi_0(t) = \frac{1}{L} \int_0^L ds \xi(s, t)$ and $\xi_{u,0}(t) = 2 \int_0^L s [\xi(s, t) - \xi_0(t)] ds$.

Equations (2.37, 2.38) give the dynamic orientation correlations and the MSD of the center of mass [15]

$$\langle \hat{\mathbf{u}}_0(t) \cdot \hat{\mathbf{u}}_0(0) \rangle = e^{-2t D_{rot}} \quad (2.39)$$

$$\langle [\mathbf{r}_0(t) - \mathbf{r}_0(0)]^2 \rangle = 2d D_{tr} t \quad (2.40)$$

where d is the dimension, $D_{rot} = \frac{\pi \zeta_s k_B T L^3}{2d}$ [34] is the rotational diffusion of a rod and D_{tr} the translational diffusion constant. The MSD of the center of mass of a treadmilling semi-flexible polymer is expected to follow a ballistic diffusion, as shown on Fig. 2.5.

We propose to include the effect of treadmilling as the kinematic terms of Eqs. (2.32, 2.33) in the above Langevin equations, such that

$$\zeta_u \partial_t \hat{\mathbf{u}}(s, t) = (\underline{\mathbf{I}} - \hat{\mathbf{u}}(s, t) \otimes \hat{\mathbf{u}}(s, t)) \cdot [\zeta_u v_p \partial_s \hat{\mathbf{u}}(s, t) + \chi_u + \xi_u(s, t)] \quad (2.41)$$

$$\underline{\zeta} \partial_t \mathbf{r}(s, t) = \underline{\zeta} v_p \partial_s \mathbf{r}(s, t) + \partial_s \chi + \xi(s, t) \quad (2.42)$$

and we obtain the equations for the mean orientation and center of mass:

$$\zeta_u \partial_t \hat{\mathbf{u}}_0(t) = (\underline{\mathbf{I}} - \hat{\mathbf{u}}_0 \otimes \hat{\mathbf{u}}_0) \cdot [\zeta_u v_p (\hat{\mathbf{u}}(L, t) - \hat{\mathbf{u}}(0, t)) + \xi_{u,0}(t)] \quad (2.43)$$

$$\underline{\zeta} \partial_t \mathbf{r}_0(t) = \underline{\zeta} v_p \frac{\mathbf{r}(L, t) - \mathbf{r}(0, t)}{L} + \xi_0(t) \quad (2.44)$$

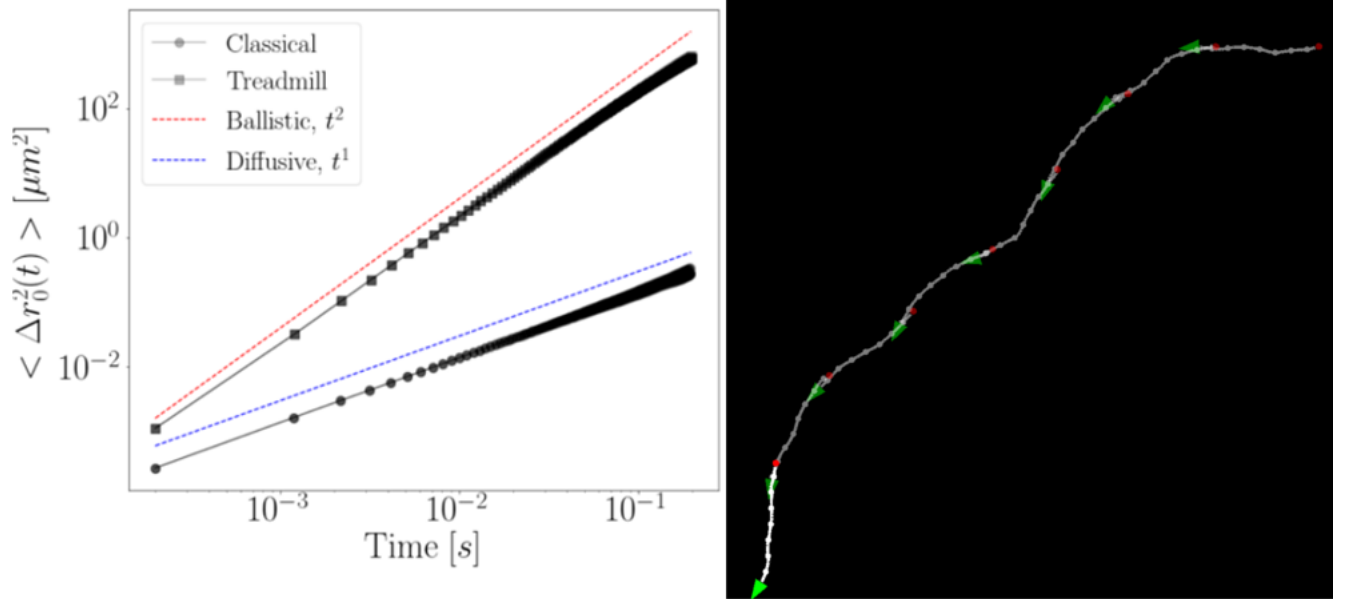


Figure 2.5: **Left** : MSD of the center of mass of classical (black circles) and treadmilling (black squares) filaments. The center of mass of the classical filament follows a diffusive power law, as predicted by Eq. (2.40), while the center of mass of the treadmilling filament follows a ballistic power law. Dashed lines are a guide to the eye for the two power laws. **Right** : treadmilling filament timelapse with regular speckles, the green (resp. the red) end is the growing (resp. shrinking) end ($t_{step} = 10^{-3}s$, $L = 8\mu m$). Speckles (white dots on the fiber) are represented for convenience, but have no physical meaning.

Chapter 3

Microrheology

3.1 Single bead passive microrheology in a pure solvent

Langevin framework is useful for the study of intracellular and microrheology properties [35]. The **Langevin Equation** is the extension of Newton's second law, but for a stochastic process, in our case for a Brownian particle. If we consider a particle of mass m , position $\mathbf{x}(t)$ at time t , we can write the following equation of motion

$$m\ddot{\mathbf{x}}(t) = -\gamma\dot{\mathbf{x}}(t) + \boldsymbol{\xi}(t) \quad (3.1)$$

where γ is a friction coefficient, given by the Stoke's law for a bead of radius R in a fluid of viscosity η : $\mathbf{F}_{drag} = -6\pi\eta R\dot{\mathbf{x}} = -\gamma\dot{\mathbf{x}}$. $\boldsymbol{\xi}(t)$ is the thermal motion, with $\langle \boldsymbol{\xi}(t) \rangle = 0$ and $\langle \boldsymbol{\xi}(t)\boldsymbol{\xi}(t') \rangle = 2\gamma k_B T \delta(t - t')$. This is the so-called Langevin equation. In cases where inertia is negligible, which is the case in most biological systems, we can write the **overdamped Langevin equation**

$$\gamma\dot{\mathbf{x}}(t) = \boldsymbol{\xi}(t) \quad (3.2)$$

The Mean Square Displacement (MSD) is defined as :

$$\langle \Delta \mathbf{x}^2(\tau) \rangle \equiv \langle [\mathbf{x}(t + \tau) - \mathbf{x}(t)]^2 \rangle_t = \int_0^T \frac{[\mathbf{x}(t + \tau) - \mathbf{x}(t)]^2}{T} dt \quad (3.3)$$

It gives us information about the spreading of a particle, if it is only due to diffusion or helped (or slowed down) by another process, for instance a viscoelastic medium. In a discrete setting, where $t = k.t_{step}$, $k = 0, \dots, n - 1$, and $T = (n - 1).t_{step}$, we can write the MSD as

$$MSD(k) = \frac{1}{n - k} \sum_{m=0}^{n-k-1} [\mathbf{x}(k + m) - \mathbf{x}(k)]^2 \quad (3.4)$$

A direct and naive calculation scales as $O(n^2)$ and is computationally too costly. Therefore we must find another method to get it with a smaller complexity. This is done using Fast Fourier Transform (FFT) on trajectory vectors, as described in [33].

If we want to know which diffusion regime the bead follows, we can compute the MSD from the overdamped Langevin equation Eq. (3.2) as

$$\langle \Delta \mathbf{x}^2(t) \rangle = \int \frac{d\omega}{2\pi} \langle \tilde{\mathbf{x}}(\omega)\tilde{\mathbf{x}}(-\omega) \rangle [1 - e^{-i\omega t}] \quad (3.5)$$

with $\tilde{\mathbf{x}}(\omega)$ the Fourier transform of $\mathbf{x}(t)$. From this, the Fourier transformed overdamped Langevin equation from Eq. (3.2) is

$$\omega^2 \langle \tilde{\mathbf{x}}(\omega)\tilde{\mathbf{x}}(-\omega) \rangle = \langle \tilde{\boldsymbol{\xi}}(\omega)\tilde{\boldsymbol{\xi}}(-\omega) \rangle = 2d \frac{k_B T}{\gamma} \quad (3.6)$$

with d the dimension (the d directions are independent in Fourier space, hence we have d times the same Fourier integral). Injecting this result in Eq. (3.5), we can solve the integral (with a contour integration, replacing ω^2 by $\omega^2 + \omega_0^2$ and taking the limit $\omega_0^2 \rightarrow 0$, see [36], Chapter 7.) such that

$$\langle \Delta \mathbf{x}^2(t) \rangle \sim 2dDt \quad (3.7)$$

where we have used the Stokes-Einstein relation $D = \frac{k_B T}{\gamma}$, and d stands for the dimension. In general, the MSD can be written as a power-law $\langle \Delta \mathbf{x}^2(t) \rangle \sim t^\alpha$. The coefficient α describes the type of diffusion regime : $\alpha = 1$ is the normal diffusion, whereas $\alpha < 1$ is a subdiffusive regime (the diffusion is "slowed down") and $\alpha > 1$ is a superdiffusive regime.

3.2 Single bead microrheology in an actin network

3.2.1 Complex Elastic Modulus

Using Langevin framework, we can extract macroscopic properties of a polymer network such as the shear modulus. From Eq. (3.2), and writing $\mathbf{x}(t)$, the position of the bead at time t , with the force-displacement relation

$$\mathbf{x}(t) = \int_{-\infty}^t dt' \chi(t-t') \mathbf{F}(t') \Leftrightarrow \tilde{\mathbf{x}}(\omega) = \tilde{\chi}(\omega) \tilde{\mathbf{F}}(\omega) \quad (3.8)$$

where $\mathbf{F}(t')$ is the instantaneous external force applied on the bead and $\chi(t-t')$ the mechanical response function, $\tilde{\mathbf{F}}(\omega)$ and $\tilde{\chi}(\omega)$ their respective associated Fourier transforms. The Langevin equation for the bead in the network can be written in Fourier space as

$$i\omega\tilde{\gamma}(\omega)\tilde{\mathbf{x}}(\omega) = \tilde{\mathbf{F}}(\omega) + \tilde{\boldsymbol{\xi}}(\omega) = \frac{\tilde{\mathbf{x}}(\omega)}{\tilde{\chi}(\omega)} + \tilde{\boldsymbol{\xi}}(\omega) \quad (3.9)$$

where $i\omega\tilde{\gamma}(\omega)\tilde{\mathbf{x}}(\omega)$ is the viscous part, $\frac{\tilde{\mathbf{x}}(\omega)}{\tilde{\chi}(\omega)}$ is the elastic part and $\tilde{\boldsymbol{\xi}}(\omega)$ is the thermal part. $\tilde{\gamma}(\omega)$ is the Fourier transform of the time-dependent friction, since we consider the general case.

The shear modulus, $G(t)$, characterizes the reponse of the material to a shear stress and it is the macroscopic quantity we want to compute. We introduce a complex shear modulus as [34] $G^*(\omega) = \int dt e^{i\omega t} G(t)$, and we assume that G^* has both storage (real) and loss (imaginary) moduli [20], such that $G^*(\omega) = G'(\omega) + iG''(\omega)$. The complex shear modulus is defined as generalizing the Stokes-Einstein Relation (GSER) to complex material [20]

$$\tilde{\mathbf{x}}(\omega) = \frac{\tilde{\mathbf{F}}(\omega)}{6\pi R G^*(\omega)} \quad (3.10)$$

Using the Force-displacement equation (3.8) it can be directly related to the response function $\tilde{\chi}(\omega)$ as

$$G^*(\omega) = \frac{1}{6\pi R \tilde{\chi}(\omega)} \quad (3.11)$$

We finally introduce the Power Spectral Density (PSD), ie: the time-averaged cross correlation function

$$C(\omega) = \int dt e^{i\omega t} \langle \mathbf{x}(t) \cdot \mathbf{x}(0) \rangle \quad (3.12)$$

where $\langle \mathbf{x}(t) \cdot \mathbf{x}(0) \rangle = \langle \mathbf{x}^2(t) \rangle - \frac{1}{2} \langle \Delta \mathbf{x}^2(t) \rangle$ up to a constant time-independent factor (see Appendix B.3). At equilibrium, the fluctuation dissipation theorem is expressed as [35]

$$C(\omega) = \frac{2k_B T}{\omega} \tilde{\chi}''(\omega) \quad (3.13)$$

with $\tilde{\chi}(\omega) = \tilde{\chi}'(\omega) + i\tilde{\chi}''(\omega)$ as for G^* . Therefore, we established a relation between the MSD of the bead and the loss modulus

$$C(\omega) = \frac{2k_B T}{\omega} \Im[\tilde{\chi}(\omega)] = -\frac{2k_B T}{6\pi R \omega} \frac{G''(\omega)}{|G^*(\omega)|^2} \quad (3.14)$$

and the storage modulus is be obtained using Kramers-Kronig relation

$$G'(\omega) = \frac{2}{\pi} \int_0^\infty d\Omega \frac{\Omega G''(\Omega)}{\Omega^2 - \omega^2} \quad (3.15)$$

3.2.2 Scaling properties

When a bead is surrounded by a network, its MSD is affected, and is related to the macroscopic properties of the network. In particular, for gels of semiflexible polymers, such as actin networks, the MSD follows three different regimes [37, 38]

$$\langle \Delta \mathbf{x}^2(t) \rangle \sim t^\alpha \quad (3.16)$$

The short times regime is characterized by the interaction of the bead with the closest actin filaments. The surrounding actin filaments form a cage where the bead is trapped and their fluctuations give an anomalous power law for the MSD, with exponent $\alpha = 0.75$, [13, 16, 28]. The long times regime corresponds to the viscous-like regime, where the MSD of the bead corresponds to the one of the medium, that is normal diffusion, so that the power law has exponent $\alpha = 1$, [16]. The intermediate times regime is characterized by the exponent $\alpha = 0.5$, [20, 37].

These different regimes can be interpreted in terms of storage and loss moduli, $G'(\omega)$ and $G''(\omega)$, which both follow the same power law [28, 39] in short-time regime

$$G'(\omega) \sim G''(\omega) \sim \omega^{3/4} \quad (3.17)$$

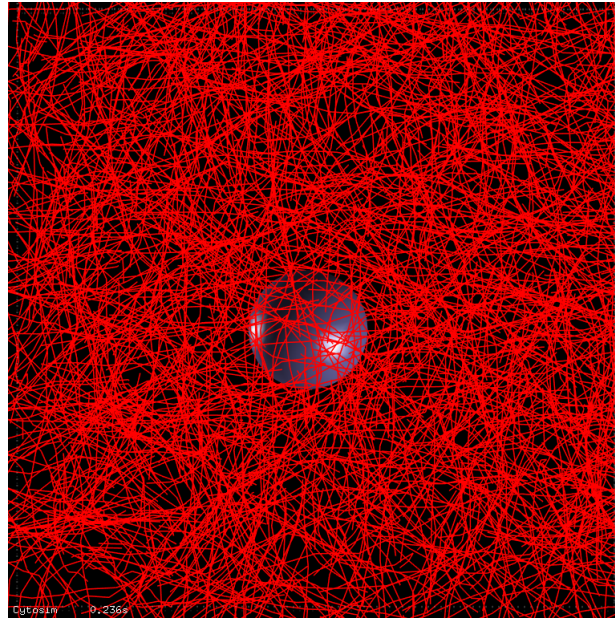
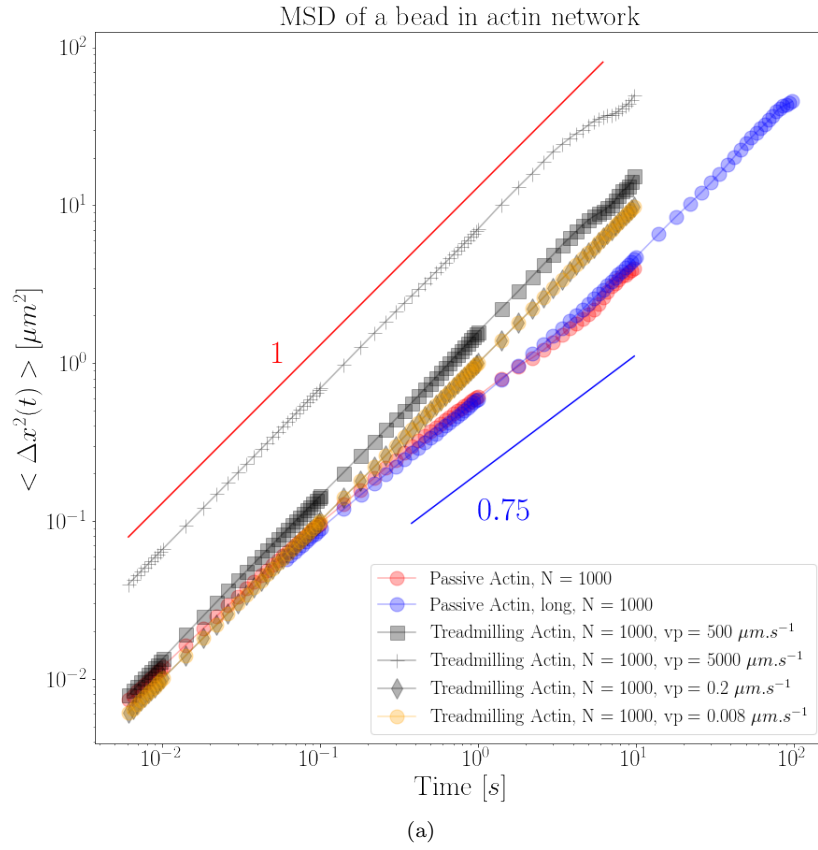
3.2.3 Simulations

First, we test single bead of radius $R = 1\mu m$ in pure water with viscosity $\eta = 0.001pN.s.\mu m^2$ at temperature $k_B T = 0.00428pN.\mu m$. We run 50 simulations with same initial conditions and parameters, in a 3D space. The MSD of the bead is computed using Fast Fourier Transform method for each simulations and is then averaged over configurations. We extract from the average the time-exponent $\alpha \approx 0.998$ and the diffusion coefficient $D \simeq 2,3.10^{-4}\mu m^2.s^{-1}$. Results are shown in Fig. 3.1.

In order to simulate microrheology of an actin network, we generate a square volume of side L with periodic boundary conditions, filled with N actin filaments of length ℓ and one bead of radius R . A Hook's law with predefined spring rigidity describes the filament-filament and bead-filament steric interactions. Simulations start from an initial state with straight filaments that relax while the bead moves due to the interactions with filament. Positions of all objects are recorded at every time step, and we extract the MSD of the bead using FFT method. Results are shown in Fig. 3.1 for an actin network with $N = 100$ filaments and a bead of radius R . We also test the effect of treadmilling at different velocities: we assume that all polymer have the same constant polymerization/depolymerization rates. We investigate four different velocities, the two lowest behaving similar to the biological treadmilling velocities.

The MSD of the bead in the passive actin network does not follow any of the predicted scaling laws, which is surprising. None of our simulations gave the expected power law for the bead MSD, either by changing the number of fibers, the constant of the steric interaction value, the size of the bead, etc. This may be due to the implementation of the bead-fiber steric interaction in Cytosim : because of the very nature of the implemented Hook's law for the repulsion, some fibers can penetrate the bead and are repelled, generating unphysical movements of the bead.

The MSD of the active networks leads to two observations: the treadmilling of polymers fluidizes the network, giving a diffusive MSD instead of the expected sub-diffusive. Besides, an increase of the treadmilling velocity increases the diffusion constant of the NSD, which corresponds to a decrease of the viscosity of the network.



(b)

Figure 3.1: **a** Mean Square Displacement of a bead of radius $1\mu m$ in pure water (blue circles) and in an actin network (black crosses, filaments of length $L = 5\mu m$, actin volume fraction $\phi = 1.5 \times 10^{-3}$) versus time ($k_B T = 0.00428 pN \cdot \mu m$, $\eta = 0.001 pN \cdot s \cdot \mu m^{-2}$). The power-law exponent of the MSD for pure solvent is $\alpha \simeq 0.998$ and the diffusion constant is $D \simeq 2,3 \cdot 10^{-4} \mu m^2 \cdot s^{-1}$. The dashed-line red power law is a guide to the eye. **b** a screenshot of an actin network, generated by Cytosim, with 1000 fibers and a bead of $1\mu m$ radius

Chapter 4

Conclusion

We have seen that Cytosim was able to simulate single semi-flexible polymer, giving the predicted dynamical scaling laws for the transverse and longitudinal amplitudes of fluctuations over several time decades. We introduced the problem of the polymerization and depolymerization for the semi-flexible filament, that has never been studied. We proposed solutions to describe the dynamics treadmilling semi-flexible polymer, as Langevin equations for the mean orientation and the center of mass that include active terms we explicated. As predicted, the MSD of the center of mass of a classical filament follows a diffusive law. The MSD of the center of mass of a treadmilling filament follows a ballistic diffusion, though it should be proved analytically. Analysis of the orientational correlations still has to be performed, to compare the effect of the treadmill to the classical case. For both, the effect of the polymerization/depolymerization speed also needs to be quantified. Besides, the Langevin equations we gave should give us predictions for the amplitudes of fluctuations of a treadmilling polymer. Further investigation on the analogy between active polymer and active brownian particles is already on.

Microrheology of actin networks was not successful, since all our simulations of actin networks gave wrong scaling laws : the MSD of the bead was diffusive, instead of being anomalous as predicted by the theory and experiments. This may be due to Cytosim itself and to the implementation of steric interactions. Therefore, we need to investigate on the implementation of the steric interaction, since the spring constant value of the interaction is arbitrary and penetration of a fiber in the bead is not physically correct. However, this will be a huge work of programming. Another solution to solve this problem may be to use the 2-bead passive microrheology. When the *in-silico* microrheology of equilibrium actin networks will give observed scaling laws, we will carefully address the treadmilling effect problem, in order to make predictions on the bulk properties of polymerizing entangled networks.

Appendix A

Langevin equation derivation

A.1 Rigid rod segments

In this section, we want to find the analytical expression of the partition function of a chain of rigid rod segments, using the maximum entropy principle [40, 41, 31].

A.1.1 Hamiltonian

Firstly, we will try to express the **partition function** of a rigid rod chain, in a discrete way. We consider a chain of $N + 1$ monomers ($\mathbf{r}_0, \mathbf{r}_1, \dots, \mathbf{r}_N$), each of mass m , interacting with the **harmonic potential** :

$$V = \frac{v_0}{2} \sum_{i=1}^N (|\mathbf{r}_i - \mathbf{r}_{i-1}| - \ell)^2 \quad (\text{A.1})$$

where v_0 is a *constant stiffness* (homogenous to a force per unit length) and ℓ is the *equilibrium distance of the points*, standing for the length of the segments. This potential does not describe the rigid rod model, but a "soft" rigidity model, useful for the calculations. However, taking the limit $v_0 \rightarrow \infty$, the constant stiffness being very large implies that the segment are effectively rigid. The first monomer, \mathbf{r}_0 is fixed at the origin, so that we remove the translational degrees of freedom, not relevant for the partition function, since the model is translationnally invariant.

Secondly, denoting $\mathbf{R}_i = \mathbf{r}_i - \mathbf{r}_{i-1}$, and considering both the kinetic and the potential energies, we end up with the following discrete **Hamiltonian** :

$$\mathcal{H} = \sum_{i=1}^N \frac{\mathbf{p}_i^2}{2m} + \frac{v_0}{2} \sum_{i=1}^N (|\mathbf{R}_i| - \ell)^2 \quad (\text{A.2})$$

The *bending stiffness* of our chain is described by the constraint :

$$\langle \mathbf{R}_i \cdot \mathbf{R}_{i+1} \rangle = \ell^2 \sigma, i = 1, \dots, N - 1 \quad (\text{A.3})$$

where σ is the stiffness parameter, equal to $\langle \cos(\theta_i) \rangle$ with θ_i the angle between \mathbf{R}_i and \mathbf{R}_{i+1} .

A.1.2 Partition function

Taking into account the constraint on the bonds (A.3), and using **Lagrange multipliers**, the **partition function** of the chain can be straightforwardly written as

$$\mathcal{Z} = \int d^{3N} R d^{3N} p \exp \left[-\beta \mathcal{H} + \sum_{i=1}^{N-1} \mu_i \mathbf{R}_i \cdot \mathbf{R}_{i+1} \right] \quad (\text{A.4})$$

where $\beta = 1/k_B T$ and $\{\mu_i\}$ are a set of Lagrange multipliers for the constraint Eq. (A.3). Using the expression of the hamiltonian (A.2) we get a simple Gaussian integral that we integrate

$$\begin{aligned}
\mathcal{Z} &= \int d^{3N} R d^{3N} p \exp \left[-\beta \sum_{i=1}^N \left(\frac{\mathbf{p}_i^2}{2m} + \frac{v_0}{2} (|\mathbf{R}_i| - \ell)^2 \right) \right] \exp \left[\sum_{i=1}^{N-1} \mu_i \mathbf{R}_i \cdot \mathbf{R}_{i+1} \right] \\
&= \int \prod_{i=1}^N d^3 p_i \exp \left[-\beta \frac{\mathbf{p}_i^2}{2m} \right] \int d^{3N} R \exp \left[-\beta \sum_{i=1}^N \frac{v_0}{2} (|\mathbf{R}_i| - \ell)^2 \right] \exp \left[\sum_{i=1}^{N-1} \mu_i \mathbf{R}_i \cdot \mathbf{R}_{i+1} \right] \\
&= \left(\frac{2\pi m}{\beta} \right)^{3N/2} \int d^{3N} R \exp \left[-\beta \sum_{i=1}^N \frac{v_0}{2} (|\mathbf{R}_i| - \ell)^2 \right] \exp \left[\sum_{i=1}^{N-1} \mu_i \mathbf{R}_i \cdot \mathbf{R}_{i+1} \right] \\
&= \left(\frac{2\pi m}{\beta} \right)^{3N/2} \left(\frac{2\pi}{\beta v_0} \right)^{N/2} \int d^{3N} R \exp \left[\sum_{i=1}^{N-1} \mu_i \mathbf{R}_i \cdot \mathbf{R}_{i+1} \right] \left(\frac{\beta v_0}{2\pi} \right)^{N/2} \exp \left[-\beta \sum_{i=1}^N \frac{v_0}{2} (|\mathbf{R}_i| - \ell)^2 \right] \\
&\xrightarrow{v_0 \rightarrow \infty} C(m, \beta, v_0) \int d^{3N} R \exp \left[\sum_{i=1}^{N-1} \mu_i \mathbf{R}_i \cdot \mathbf{R}_{i+1} \right] \prod_{i=1}^N \delta(|\mathbf{R}_i| - \ell)
\end{aligned}$$

where we used the Gaussian representation of the delta function

$$\delta(x) = \lim_{\sigma \rightarrow 0} \sqrt{\frac{1}{2\pi\sigma^2}} e^{-\frac{x^2}{2\sigma^2}} \quad (\text{A.5})$$

The term $C(m, \beta, v_0)$ is a constant that disappears when taking averages or if we consider the free energy, since it does not depend on the μ_i . Therefore we set it equal to 1.

Finally, we have

$$\mathcal{Z} = \int d^{3N} R \prod_{i=1}^N \delta(|\mathbf{R}_i| - \ell) \exp \left[\sum_{i=1}^{N-1} \mu_i \mathbf{R}_i \cdot \mathbf{R}_{i+1} \right] \quad (\text{A.6})$$

the partition function of a chain of rodlike segments, as in [10]

A.1.3 Evaluation of the partition function

The partition function (A.6) can be evaluated : the delta function imposes that $|\mathbf{R}_i| = \ell$, so we have

$$\mu_i \mathbf{R}_{i+1} \cdot \mathbf{R}_i = \mu_i \ell^2 \cos(\theta_i); d^3 R_i = \ell^2 \sin(\theta_i) d\theta_i d\phi_i$$

hence

$$\begin{aligned}
\mathcal{Z} &= \prod_{i=1}^N \int_0^{2\pi} d\phi_i \int_0^\pi d\theta_i \sin(\theta_i) \exp [\mu_i \ell^2 \cos(\theta_i)] \\
&= (2\pi \ell^2)^N \prod_{i=1}^N \left[\frac{\exp(\mu_i \ell^2 \cos(\theta_i))}{\mu_i \ell^2} \right]_\pi^0 \\
&= (4\pi \ell^2)^N \prod_{i=1}^N \frac{\sinh(\mu_i \ell^2)}{\mu_i \ell^2}
\end{aligned}$$

We can now find an expression for the Lagrange multipliers μ_i with the following reasoning : let be an averaged quantity $\langle h_k \rangle$ with average value ϕ_k . According to the maximum entropy principle [31], the average value is equal to

$$\langle h_k \rangle = \phi_k = \frac{\partial}{\partial \lambda_k} \ln(\mathcal{Z}) \quad (\text{A.7})$$

where \mathcal{Z} is the partition function and $\{\lambda_k\}$ is a set of k Lagrange multipliers.

In our case, we have, using Eq. (A.3):

$$\langle \mathbf{R}_{i+1} \cdot \mathbf{R}_i \rangle = \sigma \ell^2 = \frac{\partial}{\partial \mu_i} \ln(\mathcal{Z}) = \ell^2 \coth(\mu_i \ell^2) - \frac{\ell^2}{\mu_i \ell^2} \quad (\text{A.8})$$

hence

$$\mu_i \ell^2 = \mathcal{L}^{-1}(\sigma), \forall i = 1, \dots, N \quad (\text{A.9})$$

where \mathcal{L}^{-1} is the inverse of the Langevin function, defined as $\mathcal{L}(x) = \coth(x) - \frac{1}{x}$.

Since $\mathcal{L}^{-1}(\sigma)$ does not depend on i , the Lagrange multipliers are the same and we simply write them as μ .

A.1.4 Path integral expression of the partition function

We also write the partition function in the formalism of path integral, taking the continuum limit. First, observing that $2\mathbf{R}_{i+1}\cdot\mathbf{R}_i = 2\ell^2 - (\mathbf{R}_{i+1} - \mathbf{R}_i)^2$, and injecting it in Eq.(A.6), we have

$$\mathcal{Z} = e^{2\mu(N-1)\ell^2} \int d^{3N}R \prod_{i=1}^N \delta(|\mathbf{R}_i| - \ell) \exp \left[-\frac{\mu}{2} \sum_{i=1}^{N-1} (\mathbf{R}_{i+1} - \mathbf{R}_i)^2 \right] \quad (\text{A.10})$$

As before, the prefactor is not important, since it will disappear for averaged quantities, so we discard it. Since we're in the discrete case, we need to take the continuum limit of our model, such that

$$N \rightarrow \infty \quad \ell \rightarrow 0 \quad N\ell = L \quad \sigma \rightarrow 1 \quad (\text{A.11})$$

with L the total length of the filament. Thus the discrete vectors \mathbf{r}_i become continuous vectors $\mathbf{r}(s)$, where $s \in [0, L]$ is the arclength, and we can identify the continuous derivative as :

$$\frac{\partial \mathbf{r}}{\partial s} = \lim_{\ell \rightarrow 0} \frac{\mathbf{r}_i - \mathbf{r}_{i-1}}{\ell} \quad (\text{A.12})$$

$$\frac{\partial^2 \mathbf{r}}{\partial s^2} = \lim_{\ell \rightarrow 0} \left(\frac{\mathbf{r}_{i+1} - 2\mathbf{r}_i + \mathbf{r}_{i-1}}{\ell^2} \right)^2 \quad (\text{A.13})$$

$$\int_0^L ds \dots = \lim_{\substack{\ell \rightarrow 0 \\ N \rightarrow \infty}} \ell \sum_{i=1}^{N-1} \dots \quad (\text{A.14})$$

so, using the definition $\mathbf{R}_i = \mathbf{r}_i - \mathbf{r}_{i-1}$, we have

$$\frac{\mu}{2} \sum_{i=1}^N (\mathbf{R}_{i+1} - \mathbf{R}_i)^2 = \frac{\mu\ell^3}{2} \sum_{i=1}^N \left(\frac{\mathbf{R}_{i+1} - \mathbf{R}_i}{\ell^2} \right)^2 = \lim_{\substack{\ell \rightarrow 0 \\ N \rightarrow \infty}} \frac{\kappa}{2} \int_0^L ds \left(\frac{\partial^2 \mathbf{r}(s)}{\partial s^2} \right)^2 \quad (\text{A.15})$$

where we have defined the bending modulus κ as

$$\lim_{\ell \rightarrow 0} \mu\ell^3 \equiv \kappa \quad (\text{A.16})$$

Therefore, the partition function of Eq. (A.10) becomes the one written in Eq. (2.7).

A.2 Continuous persistent chain

A.2.1 Equivalence between discrete and continous constraints

From the discrete model, we have a set of constraints as follow :

$$\left\langle \sum_{i=2}^{N-1} \mathbf{R}_i^2 \right\rangle = (N-2)\ell^2 \quad (\text{A.17})$$

$$\langle \mathbf{R}_1^2 \rangle = \langle \mathbf{R}_N^2 \rangle = \ell^2 \quad (\text{A.18})$$

$$\left\langle \sum_{i=1}^{N-1} \mathbf{R}_i \cdot \mathbf{R}_{i+1} \right\rangle = (N-1)\ell^2 \sigma \quad (\text{A.19})$$

that can be respectively mapped in the continuous version using Eqs. (A.11) :

$$\left\langle \int_0^L ds \left(\frac{\partial \mathbf{r}(s)}{\partial s} \right)^2 \right\rangle = L \quad (\text{A.20})$$

$$\left\langle \left(\frac{\partial \mathbf{r}(s)}{\partial s} \right)_{s=0,L}^2 \right\rangle = 1 \quad (\text{A.21})$$

$$\lim_{\ell \rightarrow 0} \ell \left\langle \int_0^\ell ds \left(\frac{\partial^2 \mathbf{r}(s)}{\partial s^2} \right)^2 \right\rangle = 4pL \quad (\text{A.22})$$

where $N\ell = L$ and

$$\lim_{\substack{\ell \rightarrow 0 \\ \sigma \rightarrow 1}} \frac{\ell}{1 - \sigma} = \frac{1}{2p} = \ell_p \quad (\text{A.23})$$

is the persistence length.

Indeed, taking Eq. (A.3), and using the definition $\mathbf{R}_i = \mathbf{r}_i - \mathbf{r}_{i-1}$, we have

$$\begin{aligned} \langle (\mathbf{R}_{i+1} - \mathbf{R}_i)^2 \rangle &= \ell^4 \left\langle \left(\frac{\mathbf{R}_{i+1} - \mathbf{R}_i}{\ell^2} \right)^2 \right\rangle = 2\ell^2(1 - \sigma) \\ \ell \left\langle \left(\frac{\mathbf{r}_{i+1} - 2\mathbf{r}_i + \mathbf{r}_{i-1}}{\ell^2} \right)^2 \right\rangle &= 2 \frac{(1 - \sigma)}{\ell} \end{aligned}$$

if we now go to the continuum limit, using Eq. (A.13), we obtain

$$\lim_{\substack{\ell \rightarrow 0 \\ \sigma \rightarrow 1}} \ell \left\langle \left(\frac{\partial^2 \mathbf{r}(s)}{\partial s^2} \right)^2 \right\rangle = \lim_{\substack{\ell \rightarrow 0 \\ \sigma \rightarrow 1}} 2 \frac{(1 - \sigma)}{\ell} \stackrel{(\text{A.23})}{=} 4p \Rightarrow \lim_{\ell \rightarrow 0} \ell \int_0^L ds \left\langle \left(\frac{\partial^2 \mathbf{r}(s)}{\partial s^2} \right)^2 \right\rangle = 4p \int_0^L ds = 4pL = 2 \frac{L}{\ell_p} \quad (\text{A.24})$$

which is Eq. (A.22)

A.2.2 Continous partition function under constraints

We have four different constraints for the discrete model, so we need four different Lagrange multipliers : $\lambda, \lambda_1, \lambda_N$ and μ . Discarding all constant prefactors (with respect to space), we start with the following partition function :

$$\mathcal{Z} = \int d^{3N} R \exp \left[-\lambda \sum_{i=2}^{N-1} R_i^2 - \lambda_1 R_1^2 - \lambda_N R_N^2 + \mu \sum_{i=1}^{N-1} \mathbf{R}_{i+1} \cdot \mathbf{R}_i \right] = \int d^{3N} R e^{g(\{\mathbf{R}\})} \quad (\text{A.25})$$

Considering only the exponent in the exponential, we have :

$$\begin{aligned} g(\{\mathbf{R}\}) &= -\lambda \sum_{i=2}^{N-1} R_i^2 - \lambda_1 R_1^2 - \lambda_N R_N^2 + \frac{\mu}{2} \sum_{i=1}^{N-1} [R_i^2 + R_{i+1}^2 - (\mathbf{R}_{i+1} - \mathbf{R}_i)^2] \\ &= -\lambda \sum_{i=2}^{N-1} R_i^2 - \lambda_1 R_1^2 - \lambda_N R_N^2 \\ &\quad + \frac{\mu}{2} \left[R_1^2 + R_N^2 + 2 \sum_{i=2}^{N-1} R_i^2 - \sum_{i=1}^{N-1} (\mathbf{R}_{i+1} - \mathbf{R}_i)^2 \right] \\ &= -(\lambda - \mu) \sum_{i=2}^{N-1} R_i^2 - (\lambda_1 - \frac{\mu}{2}) R_1^2 - (\lambda_N - \frac{\mu}{2}) R_N^2 + \\ &\quad - \frac{\mu}{2} \sum_{i=1}^{N-1} (\mathbf{R}_{i+1} - \mathbf{R}_i)^2 \\ &= -(\lambda - \mu) \ell^2 \sum_{i=2}^{N-1} \left(\frac{\mathbf{r}_i - \mathbf{r}_{i-1}}{\ell} \right)^2 - (\lambda_1 - \frac{\mu}{2}) \ell^2 \left(\frac{\mathbf{r}_1 - \mathbf{r}_0}{\ell} \right)^2 - (\lambda_N \\ &\quad - \frac{\mu}{2}) \ell^2 \left(\frac{\mathbf{r}_N - \mathbf{r}_{N-1}}{\ell} \right)^2 - \frac{\mu}{2} \ell^4 \sum_{i=1}^{N-1} \left(\frac{\mathbf{r}_{i+1} - 2\mathbf{r}_i + \mathbf{r}_{i-1}}{\ell^2} \right)^2 \end{aligned}$$

and using relations (A.12, A.13, A.14), we obtain by taking the limit of the partition function :

$$\mathcal{Z} = \lim_{\substack{\ell \rightarrow 0 \\ N \rightarrow \infty \\ \sigma \rightarrow 1}} \int \mathcal{D}^3 R \exp \left[-\tau \int_0^L ds \left(\frac{\partial \mathbf{r}(s)}{\partial s} \right)^2 - \tau_0 \left[\left(\frac{\partial \mathbf{r}(0)}{\partial s} \right)^2 + \left(\frac{\partial \mathbf{r}(L)}{\partial s} \right)^2 \right] - \frac{\kappa}{2} \int_0^L \left(\frac{\partial^2 \mathbf{r}(s)}{\partial s^2} \right)^2 ds \right] \quad (\text{A.26})$$

where

$$\tau = \lim_{\substack{\ell \rightarrow 0 \\ N \rightarrow \infty}} (\lambda - \mu) \ell \quad \tau_0 = \lim_{\substack{\ell \rightarrow 0 \\ N \rightarrow \infty}} (\lambda_1, \lambda_N - \frac{\mu}{2}) \ell^2 \quad \kappa \equiv \lim_{\substack{\ell \rightarrow 0 \\ N \rightarrow \infty}} \mu \ell^3 \quad \mathcal{D}^3 R = \lim_{N \rightarrow \infty} d^{3N} x \quad (\text{A.27})$$

A.3 Langevin equation

A.3.1 Equation of motion

Considering the partition function of Eq. (A.26), we can identify the part in the exponent as the potential energy of an Hamiltonian. Until now, we discarded the kinetic part of the Hamiltonian, since it was not relevant for averaged quantities, but we want to find what is the equation of motion of our chain. Therefore, we must now include the kinetic part in our Hamiltonian and thus in the partition function :

$$\mathcal{Z}' = \mathcal{Z} \int \mathcal{D}^3 p \exp \left[-\beta \int_0^L ds \frac{p^2}{2\rho} \right] \quad (\text{A.28})$$

where ρ is the lineic mass. With these two parts (kinetics and potential) of the Hamiltonian we can write the **Lagrangian** of our system as :

$$\mathcal{L}_\tau = \int_0^L ds \frac{\rho}{2} \dot{\mathbf{r}}^2(s, t) - \int_0^L ds \tau(s, t) \left(\frac{\partial \mathbf{r}(s, t)}{\partial s} \right)^2 - \tau_0 \left[\left(\frac{\partial \mathbf{r}(0, t)}{\partial s} \right)^2 + \left(\frac{\partial \mathbf{r}(L, t)}{\partial s} \right)^2 \right] - \frac{\kappa}{2} \int_0^L ds \left(\frac{\partial^2 \mathbf{r}(s, t)}{\partial s^2} \right)^2 \quad (\text{A.29})$$

with $\mathcal{L}_\tau = \mathcal{L}_\tau(\mathbf{r}, \dot{\mathbf{r}}, t)$ and $\tau(s, t)$ a local instantaneous Lagrange multiplier [10]. The derivatives of \mathcal{L}_τ with respect to \mathbf{r} and $\dot{\mathbf{r}}$ are

$$\frac{\delta \mathcal{L}_\tau[\mathbf{r}]}{\delta \mathbf{r}} = 2(\partial_s \tau \partial_s \mathbf{r} + \tau \partial_s^2 \mathbf{r}) - \kappa \partial_s^4 \mathbf{r} \quad \text{and} \quad \frac{\delta \mathcal{L}_\tau[\dot{\mathbf{r}}]}{\delta \dot{\mathbf{r}}} = \rho \dot{\mathbf{r}} \quad (\text{A.30})$$

with boundary conditions

$$[2\tau(s, t) \partial_s \mathbf{r} - \kappa \partial_s^3 \mathbf{r}]_0^L = [2\tau_0 \partial_s \mathbf{r} \pm \kappa \partial_s^2 \mathbf{r}]_0^L = 0 \quad (\text{A.31})$$

Using the Euler-Lagrange theorem :

$$\frac{\delta \mathcal{L}_\tau[\mathbf{r}]}{\delta \mathbf{r}} - \frac{d}{dt} \frac{\delta \mathcal{L}_\tau[\dot{\mathbf{r}}]}{\delta \dot{\mathbf{r}}} = 0 \quad (\text{A.32})$$

we find the deterministic equation of motion for the chain as :

$$\rho \partial_t^2 \mathbf{r} - 2(\partial_s \tau \partial_s \mathbf{r} + \tau \partial_s^2 \mathbf{r}) + \kappa \partial_s^4 \mathbf{r} = 0 \quad (\text{A.33})$$

A.3.2 Langevin equation

We consider that the chain is in a solvent with friction ζ_s , at temperature T . We neglect the inertial terms, since we're in an overdamped regime, so $\rho \partial_t^2 \mathbf{r} = \mathbf{0}$. We must add to the deterministic equation of motion (A.33) the viscous force

$$\mathbf{F}_{drag}(s, t) = -\underline{\underline{\zeta}} \partial_t \mathbf{r}(s, t) \quad (\text{A.34})$$

where $\underline{\underline{\zeta}}$ is a friction tensor, and a stochastic force, $\boldsymbol{\xi}(s, t)$, due to the brownian motion, defined as Eqs. (2.12, 2.13). Writing the balance equation, we find the Langevin equation as Eq. 2.14

$$\underline{\underline{\zeta}} \partial_t \mathbf{r}(s, t) + \kappa \partial_s^4 \mathbf{r}(s, t) - 2\partial_s \tau(s, t) \partial_s \mathbf{r} - 2\tau(s, t) \partial_s^2 \mathbf{r}(s, t) = \boldsymbol{\xi}(s, t) \quad (\text{A.35})$$

Here, we do not include hydrodynamics in our considerations, since their contribution is logarithmic and thus negligible.

Appendix B

Scaling Laws derivations

B.1 Worm Like Chain Hamiltonian

From Eq. (A.26), we can write the associated Hamiltonian, which is the so called (continuous) WLC Hamiltonian.

$$\mathcal{H}[\mathbf{r}] = \frac{\kappa}{2} \sum_{i=1}^N \mathbf{R}_i \cdot \mathbf{R}_{i+1} = \frac{\kappa}{2} \int_0^L ds \left(\frac{\partial^2 \mathbf{r}(s)}{\partial s^2} \right)^2 \quad (\text{B.1})$$

These expressions are the discrete and continuous versions of the Hamiltonian, introduced by Kratky and Porod [7], where \mathbf{R}_i is a tangential vector, equivalent to $\mathbf{u}(s) = \frac{\partial \mathbf{r}(s)}{\partial s}$ in the continuous framework.

Using the Fourier representation of $\mathbf{r}(s)$, we have

$$\begin{aligned} \mathcal{H} &= \frac{\kappa}{2} \int_0^L ds \left(\partial_s^2 \int \frac{dq}{2\pi} \mathbf{r}_q e^{iqs} \right) \cdot \left(\partial_s^2 \int \frac{dp}{2\pi} \mathbf{r}_p e^{ips} \right) \\ &= \frac{\kappa}{2} \int_0^L ds \left(\int \frac{dq}{2\pi} (-q^2) \mathbf{r}_q e^{iqs} \right) \cdot \left(\int \frac{dp}{2\pi} (-p^2) \mathbf{r}_p e^{ips} \right) \\ &= \frac{\kappa}{2} \int \frac{dq}{2\pi} \int \frac{dp}{2\pi} (-p^2) \mathbf{r}_p (-q^2) \mathbf{r}_q \int_0^L e^{i(q+p)s} ds \\ &= \frac{\kappa}{2} \int \frac{dq}{2\pi} q^4 \mathbf{r}_q \mathbf{r}_{-q} = \frac{\kappa}{2} \int \frac{dq}{2\pi} q^4 |\mathbf{r}_q|^2 \end{aligned}$$

where we used the fact that $\int_0^L ds e^{i(q+p)s} = 2\pi \delta(p-q)$ and that the modes are not decoupled, because the Hamiltonian is real, hence they obey the relation $\mathbf{r}_{-q} = \mathbf{r}_q^*$. The Hamiltonian being quadratic, we can use the equipartition theorem $\langle H \rangle = N \frac{k_B T}{2}$. Switching to the discrete Fourier representation of $\mathbf{r}(s)$, we obtain

$$N \frac{k_B T}{2} = N \frac{\kappa}{2L} q^4 \langle |\mathbf{r}_q|^2 \rangle$$

hence

$$\langle |\mathbf{r}_q|^2 \rangle \sim \frac{L}{\ell_p q^4} \quad (\text{B.2})$$

where we used Eq. (2.9) for the persistence length ℓ_p . We can now define the mean square displacement as for Eq. (3.3) but in space, $\langle \delta \mathbf{r}^2(\ell) \rangle = \langle [\mathbf{r}(s+\ell) - \mathbf{r}(s)]^2 \rangle$ where $\langle \dots \rangle = \frac{1}{L} \int_0^L ds \dots$ is an average over the configurations.

$$\begin{aligned}
\langle \delta \mathbf{r}^2(\ell) \rangle &= \frac{1}{L-\ell} \int_0^{L-\ell} ds [\mathbf{r}(s+\ell) - \mathbf{r}(s)]^2 \\
&= \frac{1}{L-\ell} \int_0^{L-\ell} ds \left[\frac{1}{L} \sum_q \mathbf{r}_q e^{iq(s+\ell)} - \frac{1}{L} \sum_q \mathbf{r}_q e^{iqs} \right]^2 \\
&= \frac{1}{L-\ell} \int_0^{L-\ell} ds \left[\frac{1}{L^2} \sum_q \sum_p \mathbf{r}_q \mathbf{r}_p e^{i(q+p)(s+\ell)} + \frac{1}{L^2} \sum_q \sum_p \mathbf{r}_q \mathbf{r}_p e^{i(q+p)s} - \frac{2}{L^2} \sum_q \sum_p \mathbf{r}_q \mathbf{r}_p e^{i(q+p)s} e^{iq\ell} \right] \\
&= \frac{2}{L^2(L-\ell)} \left[\frac{L}{2} \sum_{q,p} \mathbf{r}_q \mathbf{r}_p (1 - e^{iq\ell}) \delta_{q,-p} \right] = \frac{1}{L(L-\ell)} \sum_q [|\mathbf{r}_q|^2 (1 - e^{iq\ell})] \\
&= \frac{1}{L(L-\ell)} \frac{k_B T L}{\kappa} \sum_q \frac{1 - e^{iq\ell}}{q^4} \\
&\stackrel{L \gg 1 \gg a}{=} \frac{1}{(L-\ell)} \frac{k_B T}{\kappa} \int_{1/L}^{1/a} \frac{dq}{2\pi} \frac{1 - e^{iq\ell}}{q^4} \sim \frac{\ell^3}{\ell_p}
\end{aligned}$$

where we integrated at first order, and we obtain the scaling relation Eq. (2.24).

B.2 Langevin equation

We may now be able to calculate the dynamical temporal scaling law of the fluctuations. Starting with the Langevin equation (A.35) for transverse fluctuations, we can set the Lagrange multiplier $\tau(s, t)$ to zero since tension is negligible in transverse directions, such that

$$\zeta_{\perp} \partial_t \mathbf{r}_{\perp}(s, t) = -\kappa \partial_s^4 \mathbf{r}(s, t) + \boldsymbol{\xi}_{\perp}(s, t) \quad (\text{B.3})$$

and using the Fourier representation of $\mathbf{r}_{\perp}(s, t)$ in frequency and wavenumber space, we find the equivalent Langevin equation in Fourier space for the transverse fluctuations

$$i\omega \zeta_{\perp} \tilde{\mathbf{r}}_{\perp}(q, \omega) = -\kappa q^4 \tilde{\mathbf{r}}_{\perp}(q, \omega) + \tilde{\boldsymbol{\xi}}_{\perp}(q, \omega) \quad (\text{B.4})$$

With Eq. (B.4), and neglecting thermal fluctuations, we can write a first scaling relation in Fourier space then in real space

$$\zeta_{\perp} \omega \sim \kappa q^4 \Rightarrow \tau_{\ell} \sim \frac{\zeta_{\perp}}{\kappa} \ell^4 \quad (\text{B.5})$$

where τ_{ℓ} is a typical relaxation time, associated to the length ℓ . Using Eq. (B.5) in Eq. (2.24), we find

$$\langle \delta \mathbf{r}_{\perp}^2(t) \rangle \sim \frac{k_B T}{\zeta_{\perp}^{3/4} \kappa^{1/4}} t^{3/4} \sim t^{3/4} \quad (\text{B.6})$$

The longitudinal amplitudes of fluctuations scale as $\langle \delta \mathbf{r}_{\parallel}^2(t) \rangle \sim t^{7/8} / \ell_p^{5/8}$ (Eq. (2.30)), so if we include friction and temperature, the scaling is

$$\langle \delta \mathbf{r}_{\parallel}^2(t) \rangle \sim \frac{(k_B T)^5}{\zeta_{\parallel}^{35/8} \kappa^{5/8}} t^{7/8} \sim t^{7/8} \quad (\text{B.7})$$

B.3 Oseen Tensor

Instead of considering a constant friction ζ_{\perp} , we may consider a local friction with the Oseen tensor as in [13], so that we can write the Langevin equation for transverse fluctuations as

$$\partial_t \mathbf{r}_{\perp}(s, t) = - \int ds' \Lambda(|s-s'|) \kappa \partial_{s'}^4 \mathbf{r}_{\perp}(s', t) + \boldsymbol{\xi}_{\perp}(s, t) \quad (\text{B.8})$$

where $\Lambda(|s-s'|)$ is the Oseen tensor, such that [34, 13, 9]

$$\Lambda(|s-s'|) = \frac{1}{8\pi \zeta_{\perp} |s-s'|} \quad (\text{B.9})$$

and its spatial Fourier transform is [42]

$$\Lambda(q) = \frac{1}{4\pi\zeta_{\perp}} \int_{\pi/a}^{\pi/L} ds \frac{\cos(qs)}{s} \stackrel{a \rightarrow 0}{L \rightarrow \infty} = -\frac{1}{4\pi\zeta_{\perp}} \left[-\gamma_E - \ln\left(\frac{1}{qa}\right) \right] \quad (\text{B.10})$$

where γ_E is the Euler constant and a is the cut-off length of our system. For $qa \rightarrow 0$, $\Lambda(q)$ diverges logarithmically. Therefore, introducing the time-dependent spatial Fourier transform of $\mathbf{r}_{\perp}(s, t)$ as $\mathbf{r}_{\perp, q}(t) = \int \frac{dq}{2\pi} \mathbf{r}_{\perp}(s, t) e^{iqs}$, we obtain the Langevin equation

$$\partial_t \mathbf{r}_{\perp, q}(t) = -\omega(q) \mathbf{r}_{\perp, q}(t) + \boldsymbol{\xi}_q(t) \quad (\text{B.11})$$

where $\boldsymbol{\xi}_{\perp, q}(t)$ is the spatial Fourier transform of the Gaussian White Noise $\boldsymbol{\xi}_{\perp}(s, t)$ and $\omega(q)$ is asymptotically [13] :

$$\omega(q) \simeq \frac{\kappa k^4}{\zeta_{\perp}} \ln \left[\frac{1}{qa} \right] \quad (\text{B.12})$$

so the long-range hydrodynamic interaction has marginal effect, and we can neglect it. We find the time dependent undulation correlation function as

$$\langle \mathbf{r}_{\perp, q}^{(i)}(t) \mathbf{r}_{\perp, -q}^{(j)}(0) \rangle = \delta_{i,j} \frac{k_B T}{\kappa q^4} e^{-\omega(q)t} \quad (\text{B.13})$$

Thus, the transverse MSD is (in 3D) the sum of two transverse components, and is, using the discrete Fourier representation

$$\begin{aligned} \langle \delta \mathbf{r}_{\perp}^2(t) \rangle &= \langle [\mathbf{r}_{\perp}(s, t) - \mathbf{r}_{\perp}(s, 0)]^2 \rangle \\ &= \left\langle \frac{1}{L^2} \sum_{q,p} \mathbf{r}_{\perp, q}(t) e^{iqs} \mathbf{r}_{\perp, p}(t) e^{ips} + \frac{1}{L^2} \sum_{q,p} \mathbf{r}_{\perp, q}(0) e^{iqs} \mathbf{r}_{\perp, p}(t) e^{ips} - \frac{2}{L^2} \sum_{q,p} \mathbf{r}_{\perp, q}(t) e^{iqs} \mathbf{r}_{\perp, p}(0) e^{ips} \right\rangle \\ &= \frac{2}{L^2} \sum_q [\langle \mathbf{r}_{\perp, q}(t) \mathbf{r}_{\perp, -q}(t) \rangle - \langle \mathbf{r}_{\perp, q}(t) \mathbf{r}_{\perp, -q}(0) \rangle] \end{aligned}$$

hence, the MSD is the sum of a static and dynamical components, so with Eq. (B.2) and Eq. (B.13), we obtain

$$\langle \delta \mathbf{r}_{\perp}^2(t) \rangle = \frac{4k_B T}{\pi \kappa} \int_{\pi/L}^{\pi/a} \frac{dq}{q^4} (1 - e^{-\omega(q)t}) \quad (\text{B.14})$$

For $t \rightarrow \infty$ the MSD saturates to the equilibrium value, such that

$$\langle \delta \mathbf{r}_{\perp}^2 \rangle \equiv \lim_{t \rightarrow \infty} \langle \delta \mathbf{r}_{\perp}^2(t) \rangle = \frac{8k_B T}{\kappa L} \sum_k \frac{L^4}{k^4 \pi^4} = \frac{2}{45} \frac{k_B T}{\kappa} L^3 = \frac{2}{45} \frac{L^3}{\ell_p}$$

with $\int \frac{dq}{2\pi} = \frac{1}{L} \sum_q$ and $\sum_{q=1,2,\dots} \frac{1}{q^4} = \frac{\pi^4}{90}$. Note that integrating for $[0, \ell]$, we recover Eq. (2.24)

Bibliography

- [1] M. C. Marchetti, J. F. Joanny, S. Ramaswamy, T. B. Liverpool, J. Prost, Madan Rao, and R. Aditi Simha. Hydrodynamics of soft active matter. *Reviews of Modern Physics*, 85(3):1143–1189, 2013.
- [2] *Molecular Biology of the Cell, 6th Edition*. Garland Science, 2014.
- [3] C. P. Broedersz and F. C. MacKintosh. Modeling semiflexible polymer networks. *Reviews of Modern Physics*, 86(3):995–1036, 2014.
- [4] D. Roberto and K. C. Holmes. NIH Public Access. *Annu Rev Biophys.*, (3):169–186, 2011.
- [5] F. Gittes, B. Mickey, J. Nettleton, and J. Howard. Flexural rigidity of microtubules and actin filaments measured from thermal fluctuations in shape. *Journal of Cell Biology*, 120(4):923–934, 1993.
- [6] A Mogilner and G Oster. Cell motility driven by actin polymerization. *Biophys. J.*, 71(December):303–3045, 1996.
- [7] O. Kratky and G. Porod. Röntgenuntersuchung geloster Fadenmoleküle. *Recueil des Travaux Chimiques des Pays Bas*, 68(12):1106–1122, 1949.
- [8] Klaus Kroy and Erwin Frey. Dynamic Scattering from Solutions of Semiflexible Polymers. *Macromolecules*, 55(3):10, 1996.
- [9] E. Farge and A. C. Maggs. Dynamic scattering from semiflexible polymers. *Macromolecules*, 34(17):6064–6073, 1993.
- [10] T. B. Liverpool and Anthony C. Maggs. Dynamic scattering from semiflexible polymers. *Macromolecules*, 34(17):6064–6073, 2001.
- [11] T. Odijk. On the Statistics and Dynamics of Confined or Entangled Stiff Polymers. *Macromolecules*, 16(8):1340–1344, 1983.
- [12] R. Everaers, A. Ajdari, and A. C. Maggs. Dynamic Fluctuations of Semiflexible Filaments. 1(3):3717–3720, 1999.
- [13] R. Granek. From Semi-Flexible Polymers to Membranes: Anomalous Diffusion and Reptation. *Journal of Physics*, 7:1761–1788, 1997.
- [14] H. Isambert, P. Venier, A. C. Maggs, F. Abdelatif, R. Kassab, D. Pantaloni, and M.-F. Carlier. Flexibility of Actin Filaments Derived from Thermal Fluctuations. *Journal of Biological Chemistry*, 270(May 12):11437–11444, 1995.
- [15] Tanniemola B. Liverpool. Dynamics of inextensible semiflexible filaments. *Physical Review E - Statistical, Non-linear, and Soft Matter Physics*, 72(2):1–15, 2005.
- [16] A. Nikoubashman, A. Milchev, and K. Binder. Dynamics of single semiflexible polymers in dilute solution. *The Journal of Chemical Physics*, 145(23):234903, 2016.
- [17] J D Ferry. Viscoelastic properties of polymer solutions. *Journal of research of the National Bureau of Standards*, 41(1):53–62, 1948.
- [18] G. H. Koenderink, M. Atakhorrami, F. C. MacKintosh, and Christoph F. Schmidt. High-frequency stress relaxation in semiflexible polymer solutions and networks. *Physical Review Letters*, 96(13):1–4, 2006.
- [19] J Käs, H Strey, J.X. Tang, D Finger, R Ezzell, Erich Sackmann, and P.A. Janmey. F-actin, a model polymer for semiflexible chains in dilute, semidilute, and liquid crystalline solutions. *Biophysical Journal*, 70(2):609–625, 1996.

- [20] Alex J. Levine and T. C. Lubensky. One- and two-particle microrheology. *Physical Review Letters*, 85(8):1774–1777, 2000.
- [21] F. Gittes and F. MacKintosh. Dynamic shear modulus of a semiflexible polymer network. *Physical Review E*, 58(2):R1241–R1244, 1998.
- [22] H. Isambert and A. C. Maggs. Dynamics and rheology of actin solutions. *Macromolecules*, 29(3):1036–1040, 1996.
- [23] Anthony C. Maggs. Two plateau moduli for actin gels. 55(6):7396–7400, 1997.
- [24] David C. Morse. Viscoelasticity of tightly entangled solutions of semiflexible polymers. *Physical Review E - Statistical Physics, Plasmas, Fluids, and Related Interdisciplinary Topics*, 58(2):R1237–R1240, 1998.
- [25] David C. Morse. Viscoelasticity of concentrated isotropic solutions of semiflexible polymers. 1. Model and stress tensor. *Macromolecules*, 31(20):7030–7043, 1998.
- [26] David C. Morse. Tube diameter in tightly entangled solutions of semiflexible polymers. *Physical Review E*, 63(3):31502, 2001.
- [27] M. L. Gardel, M. T. Valentine, J. C. Crocker, A. R. Bausch, and D. A. Weitz. Microrheology of entangled f-actin solutions. *Physical Review Letters*, 91(15):8–11, 2003.
- [28] F. Amblard, Anthony C. Maggs, B. Yurke, A. N. Pargellis, and S. Leibler. Subdiffusion and anomalous local viscoelasticity in actin networks. *Physical Review Letters*, 77(21):4470–4473, 1996.
- [29] F. Nedelec and D. Foethke. Collective Langevin dynamics of flexible cytoskeletal fibers. *New Journal of Physics*, 9:1–24, 2007.
- [30] Don S. Lemons. *An Introduction to Stochastic Processes in Physics*.
- [31] Thomas M. Cover and Joy A. Thomas. *Elements of Information Theory*. 2005.
- [32] L. Le Goff, O. Hallatschek, E. Frey, and F. Amblard. Tracer Studies on F-Actin Fluctuations. *Physical Review Letters*, 89(25):3–6, 2002.
- [33] V. Calandrini, E. Pellegrini, P. Calligari, K. Hinsén, and G. R. Kneller. nMoldyn-Interfacing spectroscopic experiments, molecular dynamics simulations and models for time correlation functions. *Collection SFN*, 12:201–232, 2011.
- [34] Masao Doi and Sam F Edwards. *The theory of polymer dynamics*. Internat. Ser. Mono. Phys. Oxford Univ. Press, Oxford, 1986.
- [35] W. W. Ahmed, E. Fodor, and T. Betz. Active cell mechanics: Measurement and theory. *Biochimica et Biophysica Acta - Molecular Cell Research*, 1853(11):3083–3094, 2015.
- [36] P.M. Chaikin and T.C. Lubensky. *Principles of condensed matter physics*, volume c. 1995.
- [37] N. Ter-Oganessian, B. Quinn, D. A. Pink, and A. Boulbitch. Active microrheology of networks composed of semiflexible polymers: Computer simulation of magnetic tweezers. *Physical Review E - Statistical, Nonlinear, and Soft Matter Physics*, 72(4):1–9, 2005.
- [38] N. Ter-Oganessian, B. Quinn, D. A. Pink, and A. Boulbitch. Active microrheology of networks composed of semiflexible polymers: Computer simulation of magnetic tweezers. *Physical Review E - Statistical, Nonlinear, and Soft Matter Physics*, 72(4):1–13, 2005.
- [39] L. Le Goff, F. Amblard, and E. M. Furst. Motor-Driven Dynamics in Actin-Myosin Networks. *Physical Review Letters*, 88(1):4, 2002.
- [40] L. Harnau, R. G. Winkler, and P. Reineker. Dynamic properties of molecular chains with variable stiffness. *The Journal of Chemical Physics*, 102(19):7750–7757, 1995.
- [41] R. G. Winkler, P. Reineker, and L. Harnau. Models and equilibrium properties of stiff molecular chains. *The Journal of Chemical Physics*, 101(9):8119–8129, 1994.
- [42] M. Abramowitz, I. A. Stegun, and D. Miller. *Handbook of Mathematical Functions With Formulas, Graphs and Mathematical Tables*, 1965.